Tephra from andesitic Shiveluch volcano, Kamchatka, NW Pacific: Chronology of explosive eruptions and geochemical fingerprinting of volcanic glass

Vera Ponomareva[1], Maxim Portnyagin[2,3], Maria Pevzner[4], Maarten Blaauw[5], Philip Kyle[6], Alexander Derkachev[7]

[1] Institute of Volcanology and Seismology, Petropavlovsk-Kamchatsky, Russia
[2] GEOMAR Helmholtz Centre for Ocean Research Kiel, Kiel, Germany
[3] Vernadsky Institute of Geochemistry and Analytical Chemistry, Moscow, Russia
[4] Geological Institute, Moscow, Russia
[5] School of Geography, Archaeology and Palaeoecology, Queen's University Belfast, Belfast, UK
[6] Department of Earth and Environmental Science, New Mexico Institute of Mining and Technology, Socorro, USA
[7] V. I. Il`ichev Pacific Oceanological Institute, Vladivostok, Russia

Submitted for publication to International Journal of Earth Sciences

Corresponding author: Vera Ponomareva

E-mail: vera.ponomareva1@gmail.com

Tel: +7 926 385 6300

Key words: explosive eruptions; tephra; volcanic glass; chronology; Kamchatka; Shiveluch

Abstract

The ~16 ka long record of explosive eruptions from Shiveluch volcano (Kamchatka, NW Pacific) is refined using geochemical fingerprinting of tephra and radiocarbon ages. Volcanic glass from 77 prominent Holocene tephras and four Late Glacial tephra packages was analyzed by electron microprobe. Eruption ages were estimated using 113 radiocarbon dates for proximal tephra sequence. These radiocarbon dates were combined with 76 dates for regional Kamchatka marker tephra layers into a single Bayesian framework taking into account the stratigraphic ordering within and between the sites. As a result, we report ~1700 high-quality glass analyses from Late Glacial-Holocene Shiveluch eruptions of known ages. These define the magmatic evolution of the volcano and provide a reference for correlations with distal fall deposits. Shiveluch tephras represent two major types of magmas which have been feeding the volcano during the Late Glacial-Holocene time: Baidarny basaltic andesites and Young Shiveluch andesites. Baidarny tephras erupted mostly during the Late Glacial time (~16 - 12.8 ka BP) but persisted into the Holocene as subordinate admixture to the prevailing Young Shiveluch andesitic tephras (~12.7 ka BP - present). Baidarny basaltic andesite tephras have trachyandesite and trachydacite (SiO_2<71.5 wt. %) glasses. The Young Shiveluch andesite tephras have rhyolitic glasses (SiO_2>71.5 wt. %). Strongly calc-alkaline medium-K characteristics of Shiveluch volcanic glasses along with moderate Cl, CaO and low P_2O_5 contents permit reliable discrimination of Shiveluch tephras from the majority of other large Holocene tephras of Kamchatka. The Young Shiveluch glasses exhibit wave-like variations in SiO_2 contents through time that may reflect alternating periods of high and low frequency/volume of magma supply to deep magma reservoirs beneath the volcano. The compositional variability of Shiveluch glass allows geochemical fingerprinting of individual Shiveluch tephra layers which along with age estimates facilitates their use as a dating tool in paleovolcanological, paleoseismological, paleoenvironmental, and archaeological studies. Electronic tables accompanying this work offer a tool for statistical correlation of unknown tephras with proximal Shiveluch units taking into account sectors of actual tephra dispersal, eruption size and expected age. Several examples illustrate the effectiveness of the new database. The data are used to assign a few previously enigmatic wide-spread tephras to particular Shiveluch eruptions. Our finding of Shiveluch tephras in sediment cores in the Bering Sea at a distance of ~600 km from the source permits re-assessment of the maximum dispersal distances for Shiveluch tephras and provides links between terrestrial and marine paleoenvironmental records.

Introduction

Correlations of individual tephra layers using geochemical fingerprinting and dating have been widely used and have applications in volcanology and various fields of paleoenvironmental research (Lowe 2011, and references herein). Tephrochronology permits reconstructing the past explosive activity of a volcano which can then be used for understanding the tectonic and magmatic processes governing the volcanic pulses (e.g., Oladottir et al. 2008). A single tephra layer or a suite of stratigraphically ordered tephra layers can serve as excellent markers which help to correlate and date various depositional successions and ensure direct comparisons between different paleoenvironmental archives (e.g., Davies et al. 2008). Correlations of tephra layers between disparate sites may, however, be complicated if several tephras from the same volcano are close in composition but dispersed in different directions from the volcano. Knowledge of all major tephra layers from a volcano, and their geochemical characteristics, can significantly improve understanding of distal tephrostratigraphy.

Andesitic tephras are considered to be difficult for geochemical identification and correlation for various reasons (e.g., Lowe 2011 and refs herein). Andesitic volcanoes commonly produce numerous and compositionally similar tephras which form complex proximal sequences. These sequences sometimes are partly eroded or only partly exposed (e.g., Donoghue et al. 2007; Turner et al. 2009). In addition, andesitic tephras often are highly vesicular and crystallized, so they may contain only tiny pockets of microlite-free interstitial glass suitable for microprobe analysis. Some microprobe glass analyses therefore might be non-representative because of entrapment of mineral phases. Even if this does not happen, glass may be compositionally heterogeneous due to magma mixing and crystallization, which makes statistical comparisons and correlations of different tephras difficult.

In spite of these problems, studies of proximal pyroclastic sequences of dominantly andesitic volcanoes are necessary for reconstructing the volcano's eruptive history and characterizing all the tephra layers that have the potential to work as marker layers in distal sites. Here we present a record of Late Glacial - Holocene explosive eruptions from the dominantly andesitic Shiveluch volcano (Kamchatka, NW Pacific). We estimate the age of the eruptions based on calibration of a sequence of 113 ^{14}C dates for proximal pyroclastic deposits and 76 dates for marker tephra layers from other volcanoes obtained elsewhere. We provide a first-order evaluation of compositional changes in the Shiveluch magmas over time based on bulk rock and glass composition in proximal pyroclastic units. Characteristics of glass from dated proximal pyroclastic units allow us to provide a set of analyses that can be used as a reference for distal correlations of Shiveluch tephras. This paper extends and refines the earlier published Shiveluch eruptive history (Ponomareva et al. 2007) and provides new insights into temporal variability of its magma compositions.

Shiveluch volcano

The andesitic Shiveluch volcano is a highly explosive eruptive center with historical (1600-ies - present) magma discharge rates of 25-30 Mt/year (Melekestsev et al. 1991), an order of magnitude higher than typical island arc volcanoes (Davidson and DeSilva 2000). Shiveluch is located ~60 km south of the northern edge of the subducting Pacific Plate and is spatially related to the junction of the Kuril-Kamchatka and Aleutian arcs (Fig. 1; Davaille and Lees 2004; Portnyagin et al. 2007). Written records of Shiveluch activity date back to AD 1739 (Gorshkov and Dubik 1970). The first large explosive eruption examined in detail occurred in 1964. It involved a sector collapse, subsequent phreatic explosion, a plinian eruption resulting in fall and pyroclastic density current deposits with a total bulk volume of 0.6-0.8 km^3, and lahars (Gorshkov and Dubik 1970; Belousov 1995). Since 1980 lava domes have been growing in the 1964 crater, occasionally producing block-and-ash and pumice flows, landslides, lahars and minor to moderate ash falls (Dvigalo 1984; Gorelchik et al. 1997; Khubunaya et al. 1995; Zharinov et al. 1995; Fedotov et al. 2004; Zharinov and Demyanchuk 2013). The most recent activity was in 2015 (http://www.kscnet.ru/ivs/kvert/volc.php?name=Sheveluch&lang=en). The frequent ash plumes from Shiveluch pose hazards to local towns and to dozens of daily air flights between North America and Far East (http://www.kscnet.ru/ivs/kvert/index_eng.php).

Since the onset of its activity over 80 ka (Pevzner et al. 2014), Shiveluch has built a composite volcanic edifice rising to over 3200 m (Fig. 1). The volcano with its debris flow plain occupies an area of ≥1300 km^2. The edifice consists of the late Pleistocene Old Shiveluch volcano which was destroyed by a collapse crater, and the currently active Young Shiveluch (YSH) eruptive center nested in the latter. The Old Shiveluch core is formed by a ~2000 m thick pile of coarse massive or weakly stratified pyroclastic deposits, probably enclosing lava domes, which is crowned with a series of lava flows erupted from four vents (Gorbach et al. 2013). The easternmost vent forms the 3283 m high Main Summit; two western vents (Baidarny vent and Southern vent) and their lava flows form Baidarny Spur (Figs. 1 and 2). Major sector collapse likely occurred in the late Pleistocene, somewhat earlier than the Last Glacial Maximum (Melekestsev et al. 1991). The resulting collapse crater has later been reshaped by numerous avalanches (Ponomareva et al. 1998; Pevzner et al. 2013). Recent studies suggest that the activity from Baidarny vents extended into the Late Glacial times (Pevzner et al. 2013).

Most of the Holocene eruptions were associated with the YSH eruptive center nested in the older collapse crater. YSH edifice is a cluster of lava domes (including the currently active one) and short lava flows. In addition, a few Holocene lava domes are located at the western slope of Old Shiveluch (Karan domes), and a tuff ring recently revealed by erosion is positioned at the southwestern terminus of the Baidarny Spur (Fig. 2; Churikova et al. 2010). The exact number of former vents within the collapse crater is not known because some of them might be covered with later deposits while others might have been destroyed by numerous debris avalanches (Ponomareva et al. 1998).

Late Glacial-Holocene erupted products from Shiveluch are mainly pyroclastic deposits (bulk volume of ~100 km^3) with subordinate amount of lava (Gorbach and Portnyagin 2011). Pyroclastic deposits on Shiveluch slopes are interlayered with paleosol horizons and provide a nearly continuous record of the volcano's activity during the last 16 ka. The older pyroclastic sequence was probably removed from the volcano's slopes by glacial erosion. Sixty prominent pyroclastic units erupted since ~11 ka have been recognized and dated (Ponomareva et al. 2007). Preserved Holocene lava flows are rare (Gorbach and Portnyagin 2011) and extend ≤4 km from vent. They are too young to be dated by radiogenic methods so their eruption ages are uncertain. The eruptive history and magmatic evolution of this tectonically important volcanic center is therefore best examined using the pyroclastic deposits.

YSH eruptions are dominated by medium-K amphibole-bearing andesites which were fairly uniform throughout the Holocene, with the exception of two large basalt - basaltic andesite eruptions (Volynets et al. 1997; Ponomareva et al. 2007). Electron microprobe analyses of rhyolitic glass from thirteen Shiveluch tephras yielded similar compositions so these tephras could not be geochemically distinguished (Kyle at al. 2011). These data gave the impression of limited variations in the magma compositions at Shiveluch during the Holocene. However, some of the YSH pumices and lavas exhibit hybrid features formed by extensive mixing of evolved and primitive magmas (Volynets 1979; Gorbach and Portnyagin 2011). They are different from Old Shiveluch (including Baidarny) rocks, which exhibit limited evidence for magma hybridism (Gorbach et al. 2013).

If the numerous tephra fall layers erupted from Shiveluch can be fingerprinted, they should make excellent markers for dating Holocene deposits and landforms up to distances of at least 350 km away from the volcano (Ponomareva et al. 2007). For example, a peat section ~80 km southeast of Shiveluch that extends back to ~6.8 ka (Pevzner et al. 1998) contains at least 28 visible tephra layers assumed to be mainly from Shiveluch. Limited microprobe analyses of Shiveluch glass, however, have permitted only a few major Shiveluch tephras to be used as markers (e.g., Braitseva et al. 1983, 1991; Bourgeois et al. 2006; Goebel et al. 2003; Kozhurin et al. 2006; O. Dirksen et al. 2011; V. Dirksen et al. 2013). On-going volcanological, paleoseismological, archaeological and paleoenvironmental research in the area (Hulse et al.

2011; Kozhurin et al 2006, 2014; Pendea et al. 2012; Pinegina et al. 2012; Portnyagin et al. 2009, 2011) would benefit if all the major tephra layers from Shiveluch are geochemically characterized, which will facilitate their use for dating and correlating various deposits and landforms.

Recent field work has permitted re-evaluation of the Shiveluch eruptive history over the last 16 ka. Recent erosion has exposed pyroclastic deposits on Shiveluch erupted between ~16 and 12 ka (Pevzner et al. 2013). These deposits were produced by weak and moderate explosive eruptions attributed to activity at Baidarny Spur based on close resemblance of bulk tephra compositions to those of Baidarny lavas (Pevzner et al. 2013). The onset of the YSH was dated at ~11.7 ka (Gorbach and Portnyagin 2011; Pevzner et al. 2013).

Proximal pyroclastic sequence

Late Glacial-Holocene pyroclastic deposits on Shiveluch include tephra fall and pyroclastic density current deposits. The pyroclastic deposits are intercalated with paleosol horizons and debris avalanche deposits and form a near-continuous record spanning the last ~16 ka (Figs. 3 - 5; Online Resource 1). The pyroclastic deposits are best exposed in deep radial valleys (Fig. 2). Typical tephra fall deposits produced by plinian eruptions of YSH are andesitic pumice lapilli tuffs (Fig. 3) with estimated bulk volumes of up to 2–3 km^3 (Ponomareva et al. 2007). Small tephras from YSH, such as those accompanying the current growth of lava dome, are composed of fine to coarse dark-pink, white, pale or gray ash. Most of these small tephras form discontinuous layers which are very similar in appearance, and are difficult to trace and correlate over the different sectors of the Shiveluch slopes.

Several basalt - basaltic andesite tephras erupted from YSH differ from the typical andesite tephra and may have been erupted from vents on the Baidarny Spur. Two major tephras were labeled the "dark package" and SHsp (Volynets et al. 1997). The "dark package" is a dark-gray stratified coarse ash of basaltic andesite composition (Volynets et al. 1997; Ponomareva et al. 2007). It was considered a main crater eruption until 2008, when its source - a tuff ring on the southwestern part of Baidarny Spur (Fig. 2) - was partly exposed by erosion (Churikova et al. 2010). The younger basaltic tephra, coded SHsp, has unique composition among the Kamchatka rocks. It is a high-K, high-Mg olivine- and phlogopite-bearing basalt (Volynets et al. 1997). Similar rocks occur in a dike on Baidarny Spur suggesting that the source of this eruption was also located at the Baidarny (Gorbach and Portnyagin 2011), however, it is not related to Baidarny or Southern vent. Four small tephras compositionally close to SHsp have recently been found and also linked to an unknown source on the western slope of Old Shiveluch (Pevzner and Babansky 2011).

Deposits of pyroclastic density currents are common at Shiveluch and are typically pumiceous ignimbrites and surge deposits. Some ignimbrites contain black scoria. Most of the ignimbrites are deposited to the south of the volcano.

Tephras from the Late Glacial Baidarny eruptive period are 1-10 cm thick layers of dull gray coarse cinders and fine ash (Fig. 4). These tephras have been found in a few outcrops at the western, eastern and southeastern slopes of the volcano. Because of the paucity of the outcrops containing these tephras and similarity of appearance and composition of these layers, we cannot correlate individual tephras between the sectors, so we refer to the whole package as "Baidarny cinders".

The Holocene YSH and Late Glacial Baidarny parts of the pyroclastic sequence are separated by ~1-1.5 meters of thinly bedded Baidarny–type cinders interlayered with 0.5-3 cm thick layers of fine to very fine white, light-gray or pink ash as well as with organic-rich paleosoils (Fig. 4c). The lower part of this succession is dominated by thin layers of ash-sized gray cinder while fine to very fine light-colored ash layers become more common higher in the succession. These tephra layers hereafter referred to as the "transition package" represent weak explosive activity related to transition from the Late Glacial Baidarny eruptive period to the YSH Holocene activity.

In addition to Shiveluch tephra, the sections around the volcano contain eight regional marker tephra layers from other Kamchatka eruptive centers (Ponomareva et al. 2007; Fig. 5), easily identified in the field based on their color, grain size, and uniform thickness, as well as numerous thin layers of dark-gray fine-grained cinders, mainly from Kliuchevskoi volcano. Together with the earlier identified marker layers from Shiveluch they divide the Holocene tephra sequence into parts and help correlate tephra sections around the volcano.

Methods

Field stratigraphy

Many YSH tephra fall deposits have distinct dispersal axes and narrow elongated area of deposition (e.g., those of the 1964 and 1854 eruptions, see Fig. 2c in Kyle et al. 2011). These tephras can only be identified in one sector of the volcano. It means that any single tephra section on the volcano's slope is not representative of the whole eruptive history, and sections from all the sectors should be measured and correlated to each other. We have measured more than 200 sections through the pyroclastic deposits around the volcano, correlated them with the help of direct field tracing and radiocarbon dating (as in Ponomareva et al. 2007), and combined them to produce a summary section (Fig. 5; Online Resource 1). In addition to the sixty pyroclastic deposits (units), reported for YSH by Ponomareva et al. (2007), we have identified thirteen more YSH pyroclastic units and examined the transition between Baidarny and Young Shiveluch activity. By unit in this paper (as well as in Ponomareva et al. 2007) we mean the pyroclastic deposits of an individual eruption clearly separated from neighbor pyroclastic layers by paleosols. The summary stratigraphy of pyroclastic deposits is the basis for the reconstruction of the Shiveluch explosive activity during the last 16 ka. Even with the extensive coverage of measured stratigraphic sections, it is possible that some tephras were missed. Also some tephras could have been miscorrelated so the presented summary section is still an incomplete record of the Late Glacial-Holocene Shiveluch eruptions, and more eruptions could be identified during further studies.

We retain the numbering and informal codes for Shiveluch eruptions and pyroclastic units proposed by Braitseva et al. (1997), Ponomareva et al. (2007) and Pevzner et al. (2013). Newly identified YSH units are marked with the number of the underlying tephra plus the letters a, b. In some cases (units 23 - 27b and bottom of the section) we were not able to correlate deposits from different slopes of the volcano, therefore we show stratigraphies from each slope separately (Fig. 5; Online Resource 1). Three units above unit 26 found on the eastern slope are labeled with letters a, b, and c, because we do not know their stratigraphic relation with units 24 and 25 found on the western slope. Four early Holocene YSH tephras stratigraphically positioned below PL1 marker tephra are placed left of the main column and labeled 61(-1)-61(-4). Units that form the transition package are labeled T1-T5. Baidarny tephras are combined into four stratigraphic/age packages (B1-B4) (Fig. 5; Online Resource 1). Yellow color indicates units with large tephra fall deposits which are likely to work as regional marker layers. In this paper we classify tephras with bulk volume >0.5 km^3 as large, 0.5–0.1 km^3 as moderate, and <0.1 km^3 as small. Dispersal axes of large tephras have been defined based on the location of the sites with their maximum thicknesses at a distance of ≤20 km from the volcano.

<u>Radiocarbon dating and calibration</u>

Proximal tephra sequences at Shiveluch contain many organic-rich paleosol layers, charcoal and wood, which have been dated with the help of radiocarbon dating. Ponomareva et al. (2007) published 101 radiocarbon dates for the proximal sequence which were roughly calibrated to determine the approximate duration of active and repose periods but an accurate calculation of the age of each eruption was not performed. Since then twelve more dates for proximal sequence have been obtained (Pevzner et al. 2013, and this study). In order to estimate the ages of the eruptions we combined all available ^{14}C dates for proximal Shiveluch deposits (a total of 113, Online Resource 1) as well as 76 dates for marker tephra layers from other volcanoes obtained elsewhere (Braitseva et al. 1993, 1995; Bazanova, Pevzner 2001; Ponomareva et al. 2013) into a single Bayesian framework (Bronk Ramsey 2009) taking into account the stratigraphical ordering within and between the sites (Online Resource 2). Units (eruptions) were treated as boundaries. The lower age boundary for the Shiveluch tephra sequence (15.8-16 ka) is based on calculations of soil accumulation rate (Pevzner et al. 2013). Whenever possible, the chronological ordering of the dates and units was defined explicitly based on stratigraphical reasoning, using the Sequence command. Separate sequences with shared markers were tied to the main sequence using OxCal's '=' linking function. Closely spaced dates and units for which the exact stratigraphical order could not be determined were put within Phases. Since the ^{14}C dates under unit 56 showed more scatter than dates above this unit, dates below said unit were assigned 5% prior outlier probabilities (the model run did not finalize without this outlier labeling). The calibration curve used was the terrestrial northern hemisphere IntCal13 (Reimer et al. 2013)

This approach has allowed us to enhance the reliability and precision of the estimated calibrated age for most of the YSH eruptions whose tephra may serve as markers over a large area as well as for the regional marker tephra layers (Fig. 5; Online Resource 3). In this paper, we use calibrated ^{14}C ages in cal BP (calibrated years before AD 1950) except for the citations from old papers where the tephra ages were given in ^{14}C yrs BP. For loose (approximate) dates we are using designation ka (calibrated kyr before AD 1950; e.g., our record spans ~16 ka).

Geochemical analysis

We have analyzed volcanic glass from 135 samples of proximal tephra-fall and pyroclastic density current deposits representing most of the identified Shiveluch eruptions (Online Resources 1 and 4). The samples were collected from outcrops around the volcano at a distance of 4-24 km from the modern dome (Fig. 2). Most of the samples are lapilli, eleven samples (mainly Baidarny cinders) are coarse to medium ash, and eight samples (mostly transition package) are fine to very fine ash (Online Resource 4). All samples were washed in distilled water and dried; lapilli were crushed. Each sample was examined under the microscope and representative unaltered glass shards were picked for the electron microprobe analysis. Backscattered electron images were obtained for representative tephra (Fig. 6).

Volcanic glass was analyzed using JEOL JXA 8200 electron microprobe equipped with five wavelength dispersive spectrometers including 3 high-sensitivity ones (2 PETH and TAPH) at GEOMAR (Kiel). The analytical conditions for glasses were 15 kV accelerating voltage, 6 nA current and 5 μm electron beam size. Counting time was 5/10 s (peak/background) for Na; 20/10s for Si, Al, Fe, Mg, Ca; 30/15 s for K, Ti, Cl, S; and 40/20 s for Mn and F. Standards used for calibration and monitoring of routine measurements were basaltic glass (USNM 113498/1

VG-A99) for Ti, Fe, Mg, Ca, P, rhyolitic glass (USNM 72854 VG568) for Si, Al, K, scapolite (USNM R6600-1) for Na, S and Cl, all from the Smithsonian collection of natural reference materials (Jarosevich et al. 1980), rhyolitic glass KN-18 (Mosbah et al. 1991) for F and synthetic rhodonite for Mn. Two to three analyses of the reference glasses and scapolite were performed at the beginning of analytical session, after every 50-60 analyses and at the end. The data reduction included on-line CITZAF correction (Armb 1995) and small correction for systematic deviations (if any) from the reference values obtained on standard materials. The latter correction did not exceed 5% relative for all elements and allowed to achieve the best possible accuracy of the data and long-term reproducibility. The INTAV intercomparison of electron-beam microanalysis of glass by tephrochronology laboratories (Kuehn et al. 2011) revealed no systematic error for glasses compositions analyzed at GEOMAR lab (coded as lab #12).

During data reduction we excluded EMP analyses with totals lower than 93 wt. %, which resulted from possible unevenness of sample surface, entrapment of voids or epoxy during analysis of very small glass fragments. Contamination by epoxy resin has also been identified by unusually high measured chlorine concentrations, which resulted from 3-4 wt. % of Cl in the epoxy resin used in the course of this study (Buehler EpoThin). Analyses contaminated by occasional entrapment of crystal phases, usually microlites of plagioclase, pyroxene or Fe-Ti oxides, were identified on the basis of excessive concentrations of Al_2O_3, CaO or FeO (and TiO_2), respectively, compared to the prevailing composition of glasses in every sample. Because volcanic glasses can be hydrated over time during post-eruptive interaction with water or contain significant but variable amount of H_2O, not completely degassed during eruption, all analyses were normalized to 100% on an anhydrous basis. The original totals measured by EMP are given in Online Resource 4.

We have obtained a total of 1688 individual glass analyses from 135 samples collected from 41 sections. Typically we made 12 analyses per sample (Online Resource 4). Two tephras (units 7 and 9) did not contain fresh glass, and four earlier identified tephras (units 17, 26, 31 and 38) have not been analyzed because the samples were not available. In order to test the applicability of our proximal data for identification of distal tephras, we have also used 70 individual glass analyses for distal tephras obtained under the same analytical conditions (Online Resource 5). In discussion, we also used 63 XRF and 22 wet chemistry analyses reported by Ponomareva et al. (2007) and seven new XRF analyses on bulk Baidarny and YSH tephra (Online Resource 6). All analyses of bulk tephra have been performed on pumice or cinder lapilli so they have not been influenced by eolian segregation and should be representative of bulk magma composition.

Results

<u>Stratigraphy and ages of analyzed pyroclastic deposits</u>

Fig. 5 presents a summary stratigraphy of proximal Shiveluch pyroclastic units and their calibrated ages. Stratigraphic position of all the geochemically characterized samples and all the radiocarbon dates for the proximal pyroclastic sequence are provided in Online Resource 1. Most of the dates are in good agreement with the stratigraphy except for one case discussed below. The section also includes marker tephra layers from other volcanoes. The 76 radiocarbon dates for the marker tephra layers are placed in the Online Resource 2 (Oxcal code). One ^{14}C date (9310±80) on a bulk sample below the PL1 marker tephra contradicts a new high quality date of 10,080±40 for this tephra obtained elsewhere (Ponomareva et al. 2013) and makes the ages of the units in this part of stratigraphy somewhat younger. We, however, retain all the published dates in order to avoid arbitrary selection of the "good" dates.

<u>Bulk compositions of Shiveluch tephra</u>

Typical YSH pumice is light gray or light-yellow to tan, highly vesicular lacy andesite with fluidal textures and 20-50% of phenocrysts (Fig. 6a-c). General mineral assemblage of andesitic YSH tephra includes plagioclase, green hornblende, magnetite, ilmenite, ortho- and clinopyroxene in various proportions. Some tephras (e.g., SH_3, SH_5) contain brown hornblende. Olivine and apatite may occur as accessory minerals. YSH and Baidarny cinders are gray to dark-gray, highly crystallized vesicular basalts - basaltic andesites abundant in microlites (Fig. 6d-f). "Dark package" cinders have the most massive and dense particles with rare rounded vesicles (Fig. 6e). Overall, basalt - basaltic andesite cinders are more crystallized than andesitic pumice and many of them contain only tiny (≤5 μm) pockets of interstitial glass. Mineral assemblage of the cinders is dominated by olivine, clinopyroxene and plagioclase. Tephra SHsp (unit 28; Fig. 6d) contains phenocrysts of olivine, clinopyroxene, mica and green hornblende.

Late Glacial - Holocene Shiveluch lapilli are predominantly andesites and basaltic andesites of medium-K compositions (Ponomareva et al. 2007; Fig. 7). SHsp tephra has K_2O contents >1.6 wt. % and is a high-K basalt very different from the rest of the pyroclastic deposits (Fig. 7) (Volynets et al. 1997). Compositions of the pyroclastic deposits overlap closely with the YSH and Baidarny lavas (Gorbach and Portnyagin 2011), although lava represents only a few short periods of activity whereas the pyroclastic deposits were formed in over 80 eruptions spanning the last ~16 ka (Fig. 7; Online Resource 1). Late Glacial Baidarny cinders have distinctively higher TiO_2, Al_2O_3 and Na_2O, and lower MgO contents at given SiO_2 compared to the YSH tephra (Fig. 7), and are similar to the compositions of lavas from the Baidarny and Southern vents (Gorbach et al. 2013). Very tight and linear trends of the YSH pumice and lava compositions on variation diagrams of major elements are argued to originate via fractional crystallization and concurrent mixing of mafic and silicic magmas as well as via crystal accumulation in evolved melt (e.g., Dirksen et al. 2006; Humphreys et al. 2008; Gorbach and Portnyagin 2011; Gorbach et al. 2013).

Volcanic glass compositions

Volcanic glass compositions from all Shiveluch tephra range from ~58 to 80 wt. % SiO_2 and fall into two major groups: low- and high-Si (Figs. 8 and 9). Glasses from Baidarny cinders have predominantly trachyandesitic and trachydacitic compositions with 62-71.5 wt. % SiO_2 ("low-Si glasses" further on). Glasses from YSH tephras are mostly rhyolitic with SiO_2=71.5-80 wt. % ("high-Si glasses" further on). Some low-Si glasses (58-71.5 wt. % SiO_2) also occur during the YSH activity, mostly in minor and moderate eruptions, and in two large basalt - basaltic andesite tephras units 28 (SHsp) and 46 ("dark package"). Most of these glasses fall into trachyandesitic and trachydacitic fields with subordinate amount of glass compositions in the upper part of the dacite field. Both trachydacitic and rhyolitic glasses are equally present in small tephras from the transition package.

On Harker variation diagrams Shiveluch glasses exhibit well-defined trends of decreasing FeO, TiO_2 and MgO contents with decreasing SiO_2 (Fig. 9). Na_2O contents reach maximum at SiO_2 of ~65 wt. % and then decrease with increasing SiO_2. K_2O increase and Al_2O_3 and CaO decrease with increasing SiO_2 but are more scattered compared to other major elements. On the K_2O-SiO_2 diagram the majority of rhyolitic glasses falls into the medium-K field (Fig. 9) with K_2O contents between 2.4 and 3.7 wt. %, the range being larger than that of 2.5-3 wt. % identified by Kyle et al. (2011) for thirteen YSH tephras. A small population of high-K (K_2O>4 wt. %) rhyolitic glasses is found in small tephras from the transition package.

Low-Si glasses from Shiveluch have medium- to high-K compositions. Baidarny glasses form a trend from ~62 to 71 wt. % SiO_2. Glasses from YSH units 43 and 46 ("dark package") fit into the same trend but also include glasses with lower SiO_2 contents (60-62 wt. % SiO_2). The lowest SiO_2 contents (58-60 wt. %) occur in glass from unit 61(-2) stratigraphically positioned below PL1 marker tephra (Fig. 5; Online Resource 1). Glasses from Baidarny and three above mentioned units 43, 46, and 61(-2) are higher in alkali and lower in CaO contents than glasses from most of the other YSH cinders; only a few of the latter partly fit into the Baidarny-dark package trend with the glasses from unit 36a being the closest. Glasses from SHsp and similar minor tephra (unit 36b) stand apart from other Shiveluch glasses and have distinctly high-K glass with highly variable K_2O contents (3.69-5.96 wt. %) and SiO_2 range between 59.8 and 66.9 wt. % in SHsp tephra.

The majority of the YSH andesitic tephra units have quite homogeneous (SiO_2 variations within 2 wt. %) rhyolitic glass compositions (Fig. 10a); a few have variable glass compositions usually organized in trends or in different populations (Fig. 10b). On Harker variation diagrams homogeneous glasses form individual clusters: some of those differ in K_2O and/or other oxides from each other while the others have overlapping compositional fields (Fig. 10a). Among the heterogeneous glasses, the most pronounced variations in SiO_2 contents (64-74 wt. %) are observed in SHdv fall deposits (unit 34) (Fig. 10b); shorter trends are characteristic for tephra from units 6 (SH_2), b, 56, 57 and some others. Mixed material with two or three glass populations occurs in some ignimbrites (Online Resource 4). Most of Baidarny cinders have slightly variable glass compositions forming trends in the trachyandesitic - trachydacitic field (Fig. 9).

Temporal variations of glass composition in Shiveluch tephra

Low-Si glass compositions predominated during the Late Glacial activity between ~16 and 12.8 ka. In products of Holocene eruptions, low-Si glasses occur a number of times, most frequently between ~4 and 8.4 ka, when the YSH andesitic eruptions were relatively rare (Fig. 11). High-Si glasses typical for the YSH activity first appeared at ~12.7 ka in thin layers of fine to very fine white ash in the transition package. During the YSH lifetime, the compositions of high-Si glasses have exhibited alternating periods of decreasing or increasing SiO_2 (Fig. 11). Well expressed periods of decreasing SiO_2 took place at ~11-9.9, 8.5-7.7, 5.6-4.9 and 4-3 ka, and 1.5 ka-present (except for AD2001 glasses). Increasing SiO_2 was characteristic for periods of ~9.9-8.5, 4.9-4, and 2.9-1.5 ka. The systematic changes of SiO_2 resulted in semi-continuous wave-like pattern of glass compositions through time (Fig. 11).

Variations of other major element oxides strongly correlating with SiO_2 content in Shiveluch glasses (MgO, FeO, TiO_2, CaO, Al_2O_3) also exhibit a wave-like pattern through time. Variations of K_2O in glasses are somewhat different from other major element oxides (Fig. 11). Among the large tephras (except for the SHsp), the most high-K glass compositions come from vitreous tephras erupted during the initial stages of the YSH activity between 11.1 and 8.4 ka (Figs. 9 and 11). The majority of these high-Si glasses have $K_2O>3$ wt. % whereas glasses from more recent eruptions (8.4 - 1.8 ka) have predominantly <3 wt. % K_2O.

The significant variability of Shiveluch glasses suggests that many of the units can be discerned from each other based on their glass compositions. The wave-like changes of major oxides through time, however, indicate that (1) some glass compositions may be repeated within different time intervals, and (2) glasses from the neighbor units in the stratigraphic succession may have very similar compositions.

Discussion

Comparison of Shiveluch tephra compositions to those from other Kamchatka tephra

Proximal YSH bulk lapilli have high MgO (2.3–6.8 wt. %), Cr (47–520 ppm), Ni (18–106 ppm) and Sr (471–615 ppm) and low Y (<18 ppm) (Ponomareva et al. 2007). These features distinguish YSH erupted products from other Kamchatka Holocene pyroclastic deposits. Some of these features have also been described for bulk samples of distal YSH tephra and used for correlations of distal tephra layers. Braitseva et al. (1997) reported high Cr (98-124 ppm), Ni (26-30 ppm) and Sr (415-461 ppm) and low Y (12-13 ppm) in two samples of the YSH fine ash. Kyle et al. (2011) proposed Cr contents of >50 ppm (the highest among other silicic tephras in Kamchatka) and La/Yb ratio of 4-10 as the most diagnostic characteristics for identifying YSH bulk distal tephra.

For identification of distal tephras, however, results derived from bulk compositions may be inconclusive because of eolian differentiation and contamination with terrigenic material. Volcanic glass is the predominant component of most tephras and its composition is normally used for chemical fingerprinting and distal correlations of tephra (e.g., Lowe 2011). The main major element characteristics of the YSH rhyolitic glass reported earlier is medium K_2O contents (2.5–3.0 wt. %) (Kyle et al. 2011). This is clearly not enough to identify Shiveluch tephra in distal localities which is why Kyle et al. (2011) suggested complementing glass data with the trace element data on bulk samples.

Our new data allow us to further refine specific features of Shiveluch glasses, which help to discern Shiveluch pyroclastic deposits from other major Kamchatka tephras. Shiveluch glasses have characteristically high Na_2O, low CaO and consequently low $CaO/(Na_2O+K_2O)$ at any given SiO_2 (Fig. 12a) corresponding to calc-alkaline series in classical definition of Peacock (1931) [$CaO/(Na_2O+K_2O)<1$ at $SiO_2=60$ wt. %]. Unlike Shiveluch, many other Kamchatkan volcanoes produced glasses which belong to calcic series. Such glass compositions are characteristic for major tephras from Avachinsky, Iliinsky and Ksudach volcanoes (Fig. 12a). Noticeably, Shiveluch bulk rock compositions also have the strongest calc-alkaline specifics compared to other volcanoes in the Central Kamchatka depression and likely in all Kamchatka (e.g., Portnyagin et al. 2007).

The strong calc-alkaline affinity is, however, not a unique feature of Shiveluch glasses. Glasses from some other major silicic and intermediate tephras in Kamchatka also fall into, or close to the Shiveluch field on the $CaO/(Na_2O+K_2O)$ vs. SiO_2 diagram (Fig. 12a). These are glasses from KHG, KHD, KRM, KO, KZ, OP, and OPtr marker tephras (Kyle et al. 2011) overlapping with high-Si Shiveluch glasses, and those from Plosky volcano (Ponomareva et al.

2013) overlapping with intermediate Baidarny glasses. KHD and KO glasses have lower, and those of OP and OPtr – higher K_2O content than Shiveluch glasses at given SiO_2 (Table 1; Fig. 12b). Medium-K glasses from KZ tephra are distinguished by their elevated CaO (>1.5 wt. %). Glasses from KRM tephra have elevated Cl (>0.20 wt. %) and those from KHG – low Cl (<0.08 wt. %) contents (Fig. 12c). Intermediate Baidarny glasses can be distinguished from those of Plosky volcano on the basis of high K_2O, low Cl (<0.1 wt. %) and high P_2O_5 (>0.5 wt. %) contents in the latter (Fig. 12, Table 1). Thus, strongly calc-alkaline medium-K characteristics of Shiveluch glasses along with moderate Cl, CaO and low P_2O_5 allow reliable discrimination of silicic Shiveluch tephras from the majority of other large Holocene tephras of Kamchatka.

Identification of Shiveluch tephra in distal localities and their correlations to proximal tephra units

The majority of distal Shiveluch tephras have equivalent proximal pumice fall deposits (Braitseva et al. 1997; Ponomareva et al. 2007). Fingerprinting of these proximal units, therefore, is most important in order to provide a reference for correlations with distal tephra. Two Holocene basalt - basaltic andesite tephras (SHsp and dark package) were also dispersed over large areas (Volynets et al. 1997) and are important for the reference set. Some YSH small tephras like the 2010 ash (Ponomareva et al. 2012) or co-ignimbrite fall deposits may also form distinct layers over the distances of 80 km so their compositions should also be considered. The dispersal of Baidarny cinders is not mapped but based on their proximal thicknesses (Fig. 4) and field tracing they may well be found over 30 km from the volcano.

Some YSH tephras have been recognized on Bering and Attu Islands and at Okhotsk coast of Kamchatka (Figs. 12d and 13), ~350-850 km to the east and 400 km southwest from the volcano (Kirianov et al. 1990; Melekestsev and Kurbatov 1998; Pevzner 2003, 2010; Kyle et al. 2011). Such distal findings, however, are few because of the proximity of the seas in the east and paucity of measured terrestrial sections in the northern and western directions from the volcano. In addition, most of these correlations were based on field tracing and ^{14}C dating and only very few were supported by microprobe glass analyses (Kyle et al. 2011; Dirksen et al. 2011).

At distances of 100-200 km from the volcano, typical andesitic YSH tephra is coarse to fine-grained ash of specific "salt-and-pepper" color where "salt" consists of pumiceous grains and/or plagioclase and "pepper" – of dark-colored minerals (Braitseva et al. 1997). This is consistent with the crystal-rich nature of the YSH magmas. Farther downwind these tephras normally still retain visible grains and do not acquire significant amount of very fine ash. These distal tephras mainly correlate with non-graded proximal pumice layers with distinct dispersal axis. Bulk composition of YSH tephra normally changes downwind from andesite (lapilli) to basaltic andesite (coarse ash enriched in mineral grains) and then to andesite-dacite (dominantly vitric fine ash) (Braitseva et al. 1997). Isopach maps or areas of dispersal have been published for thirteen YSH andesitic tephras (Kyle et al. 2011) and for two major YSH basalt - basaltic andesite tephras ("dark package" and SHsp, units 46 and 28, respectively) (Volynets et al. 1997).

We have characterized glass from most of proximal large pyroclastic deposits geochemically, refined their ages, and shown their main dispersal sectors and axes (Fig. 5; for orientation the north-based directions are labeled on Fig. 2). All data are compiled in Online Resource 4, which provides a practical tool for comparison of glass compositions from unknown tephra with our database of Shiveluch proximal glasses. This file contains description page; our complete data set of Shiveluch EMP glass compositions from proximal tephras; sheet with calculated mean compositions of glasses from Shiveluch units and data on their ages and dispersal; sheet to enter user’s data; two sheets for comparing unknown tephra with Shiveluch glasses (SC-test and t-test); service tables; sheets SC matrix and SC matrix (large) located at the end of the table. Data on the large tephras dispersal are given in the sheet named "all average". Those include dispersal sectors at a distance of ≤20 km from the volcano (in degrees from north clockwise) and main dispersal axes based on the maximum thickness of each tephra at the same distance. These axes are also indicated on Fig. 5 and in Online Resource 1.

Our comparison with Shiveluch glasses is performed using two alternative approaches: similarity coefficient and statistical *t*-test. The similarity coefficient (SC) between two mean compositions is calculated following a formulation by Borchardt et al. (1972) commonly used in tephrochronology (e.g., Lowe 2011; Davies et al. 2012). SC is calculated for 10 elements (Si, Ti, Al, Fe, Mg, Ca, Na, K, P, Cl) and for all Shiveluch units compared to unknown glass. Optionally, P can be excluded from the calculations when its concentration approaches detection limit of microprobe analyses and thus can influence SC significantly. Mn is not included in calculations because this element correlates strongly with Fe, has low concentrations in glasses and is usually determined with relatively low precision. According to Froggatt (1992) two analyses are considered to be equivalent when SC >0.92.

The statistical *t*-test (Microsoft Excel) is performed for the case of two-tail unequal distribution for 11 elements. The null-hypothesis of inequality is rejected at critical *t*-value of 0.05. The number of elements for which the null-hypothesis is rejected defines T_{11} value. The higher the T_{11} value the more similar are two mean glass compositions. In practice, very similar glasses have T_{11} >6, that is, means for 6 elements of 11 in consideration are statistically indistinguishable on 95% confidence level.

Both tables calculating SC and *t*-values have options for "fine tuning" allowing to narrow the searchable database. For example, when working with thick Shiveluch layers at distant localities it can be reasonable to exclude minor eruptions. Entering the direction to the sampling site from Shiveluch allows one to further exclude eruptions that sent tephra in other directions. Another very effective way to narrow an age interval is to provide any age constraints available from direct dating of the deposits or from stratigraphy. Finally, settings of critical SC and T_{11} values can be changed to higher or lower values. Based on our testing, the tables are effective in defining one or a few Shiveluch eruptions which fit all above mentioned criteria. In everyday work with the database, it is quite common that both SC and *t*-test point to one Shiveluch eruption as an ultimate source of unknown tephra. Below we describe examples of a few long-distance correlations done with the help of the new database and major conclusions derived from these results.

Sheets SC matrix and SC matrix (Large) located at the end of the Online Resource 4 show Shiveluch units which are similar in glass compositions. Two large basalt - basaltic andesite tephras, SHsp (unit 28) and "dark package" (unit 46) have unique compositions and can be used as markers in distal localities. From 41 large pumiceous tephras, only few have unique glass compositions: 14, 15, 34 (SHdv), 45, 47, 55. All others have more or less strongly expressed geochemical similarity to some other YSH units, and their identification in distal sites requires further constraints from stratigraphy, age and dispersal axes. Proximal glass data, however, provides new compositional constraints which help to reduce the correlation uncertainty.

Examples of long-distance correlations of Shiveluch tephra

Based on our data for major proximal YSH tephras including their ages, glass chemistry, and stratigraphic position between regional marker tephra layers, we can now ascribe some "unknown tephras" analyzed on-land and in marine cores to YSH. Here we provide a few examples of such correlations, which allow us to better estimate the distance of dispersal of the largest YSH tephras and provide the basis for estimates of tephra volumes and magnitudes of the eruptions. These data also demonstrate practical results of using our new database of proximal Shiveluch glasses (Online Resource 4).

1. Fine-grained tephra dubbed "Lower yellow" (LY) was long known in the Eastern volcanic front between Kronotsky volcano and Bolshoi Semiachik caldera (Fig. 13). It was locally dated at ~9300 ^{14}C yrs and used for dating of volcanic features at Krasheninnikov and Kikhpinych volcanoes (Braitseva et al. 1989; Ponomareva et al. 1990). The source of this tephra was not known although sources of major silicic tephras had already been identified by this time (Braitseva et al. 1995, 1997). Microprobe analyses of glass have allowed us to identify the same tephra on the slopes of Kliuchevskoi volcano where it was medium sand size (Fig. 14a; Portnyagin et al. 2011). In both areas, the glass was characterized by high Na_2O contents typical

for Shiveluch, but it had lower SiO_2 and higher K_2O contents than then known for Shiveluch tephra, and did not fit into the geochemical portrait of tephra from any other volcano (Kyle et al. 2011). With our current extensive coverage for the proximal Shiveluch tephra, we can identify the "LY" as one of the YSH early Holocene tephras (Figs. 10a and 14a). Comparison of glass compositions from each of the "LY" samples to the proximal YSH dataset shows that up to three large YSH tephras may geochemically match it. Consideration of dispersal axis (southwards) and age interval (early Holocene), however, allows us to single out unit 58 as the most probable match (SC_{10} values of 0.929-0.961, and T_{11} of 6-8). The resulting distribution map (Fig. 13) prompts that "Lower yellow" is one of the larger eruptions from Shiveluch.

2. SH_5 tephra is one of the markers from YSH dispersed to the south of the volcano (Braitseva et al. 1997). Its previous age estimate was based on erroneous correlation of distal tephra dispersed to the south with the proximal tephra unit 24 at the northwestern slope of the volcano dated at ~2550 ^{14}C yrs (Ponomareva et al. 2007). By comparing the glass data for both tephras, we were able to untangle the proximal stratigraphy and correlate the distal tephra to YSH unit 21 dated at ~1850 cal BP (Fig. 14b). Comparison of glass compositions from distal SH_5 tephra and unit 21 yielded high SC_{10} (0.953) and T_{11} (10) values while comparison of the same tephra to unit 24 yielded SC_{10} (0.918) and T_{11} (4). The younger age for the SH_5 tephra allows us to reconsider the ages of many important volcanic events in the Kliuchevskoi volcanic group whose ages have been estimated relative to SH_5: Bezymianny eruptive period BI with its largest explosive eruption (Braitseva et al. 1991); eruption of the Kliuchevskoi famous high-Mg cinder cones (Auer et al. 2009), active period in the Tolbachik monogenetic lava field (Braitseva et al. 1983), etc.

3. Very fine rhyolitic hornblende-bearing ash was found in two cores at the Shrishov Ridge (Bering Sea) in association with the early Holocene PL2 cindery tephra from Plosky volcano, which serves as a marker in the summary Shiveluch section and fits between units 56 and 57 (Fig. 5) (Ponomareva et al. 2013). Rhyolitic glasses in both cores correspond to calc-alkaline medium-K rhyolites with moderate Cl and CaO, and low P_2O_5 contents, which is consistent with their origin from YSH (Online Resources 4 and 5). In the core SO201-2-77KL (Fig. 13; N 56.3305° E 170.6997°), both PL2 tephra and YSH glasses are found at the depth of 116-117 cm. Formal comparison of rhyolitic glass from this layer to the proximal dataset (Online Resource 4) shows that it passes the test for similarity with the glasses from units 51, 54 and 56 with the best match to unit 56 (SC_{10}=0.965 and T_{11}=10) (Fig. 14c). Considering its stratigraphic proximity to PL2 tephra in the proximal sequence, unit 56 is likely the source of this marine ash (Fig. 14c).

In the core SO201-81KL (pilot) (N 56.7165° E 170.4962°) rhyolitic glass was found at the depths of 10-13 and 14-17 cm in association with PL2 tephra, which is more abundant in the lower sample (Ponomareva et al. 2013). Rhyolitic glasses have typical YSH medium-K composition (Fig. 14c). It is not clear whether all these glasses come from a single eruption or belong to several different units. As a single unit, these glasses compositionally match five large YSH tephras (units 1, 4, 6, 27, and 36). All these units, however, are younger than ~5.6 ka. Taking into account a close association of the glasses with PL2 tephra dated at 10.2 ka, we tend to favor unit 59 (10.7 ka) with dispersal axis to the east as a correlative for at least glasses from the 14-17 cm level (T_{11}=8) (Fig. 14c). Other glasses may belong to different units.

Exact correlations of submarine tephra to certain YSH units require more analytical work on the former, but it is important that at least two different early Holocene YSH tephras were found at a distance of 560-580 km away from the source. These are the first ever findings of Shiveluch tephra in marine cores. Presence of different tephras in the same layers in the marine cores may result from low accumulation rate of the sediments and/or contamination during the coring of semi-liquid Holocene deposits.

4. Kyle et al. (2011) attributed three tephra samples (95-01/1, 95-01/2 and 95-06/1) collected on Attu Island (western Aleutians) to YSH (Fig. 13). If this correlation is correct, it would increase the estimates of dispersal distance for Shiveluch tephra from 350 km (Ponomareva et al. 2007) or 560-580 km (see above) to 850 km. The three samples are very close geochemically (Fig. 14d). All of them fit into an age interval of ~3000-5100 ^{14}C yr BP (Kyle et al. 2011). The Attu tephras have lower K_2O contents than the majority of the YSH glasses (Fig. 14d). Only one of those samples (95-01/2) passed the formal test on similarity with any of the proximal units, however, a probable match (unit 6) is far younger (764 cal BP) and has a SSW- and not E-directed dispersal axis. At this stage correlation of the Attu tephras with Shiveluch is tenuous and we leave open the possibility that these tephras may have come from some closer source in the Aleutians.

Geochemical variability of Young Shiveluch glasses

Significant geochemical variability of glasses from the YSH tephras, which facilitates their usage in tephrochronology, is rather unexpected result given the relatively short time interval of the volcanic activity (Holocene) and earlier data by Kyle et al. (2011) who reported a rather small compositional variability of Shiveluch glasses. It is therefore worthwhile to analyze possible petrological reasons for the compositional variability of glasses and rocks documented in our study.

Here we refer to pyroclastic and effusive Shiveluch rocks as close compositional analogues of magmas that existed at depth and have undergone degassing upon eruption. Volcanic glasses represent a (partially) degassed residual melt quenched during eruption. The glasses can approach the composition of melt in magma chamber or be more evolved due to late crystallization, which may occur immediately before eruption and during magma transport to the surface (e.g. Blundy and Cashman 2001). The compositions of YSH rocks and glasses can thus be interpreted in terms of a number of petrogenetic processes including: 1) crystallization, 2) crystal removal, sorting or accumulation, 3) mixing of variably fractionated magmas, and 4) mixing with magmas of different geochemical type. The relative role of these processes in the petrogenesis of YSH lavas was discussed by Gorbach and Portnyagin (2011) and Gorbach et al. (2013).

Crystallization is a major petrogenetic process occurring either due to magma cooling or decompression and water degassing from magma (e.g., Eichelberger 1995; Blundy et al. 2006; Portnyagin et al. 2012). In most Shiveluch magmas, crystallizing assemblage of minerals is represented by ortho- and clinopyroxene, plagioclase, hornblende, oxides and apatite (Gorbach and Portnyagin, 2011). Effects of crystallization of this low-Si and low-K assemblage are clearly seen in the composition of glasses, which often exhibit short (SiO_2 range of 2-3 wt. %) but well defined trends of coherently increasing SiO_2 and K_2O as crystallization proceeds (Fig. 10b). Crystallization of magma results in evolving melt and increasing amount of crystals but has no effect on bulk magma composition and thus can be suggested for tephras of identical bulk composition with different composition of glasses.

Processes of crystal removal, sorting and accumulation are related to physical movement of crystals relative to melt and each other, and therefore they have no effect on the composition of melt but are able to change proportion between the melt and amount of crystals in magma. For example, Gorbach and Portnyagin (2011) showed that compositional trend of Young Shiveluch lavas can be well explained by selective separation of mafic minerals, primarily, hornblende and oxides relative to plagioclase.

Processes of *mafic and evolved magma mixing* are well documented for YSH lavas and pyroclastics (Volynets 1979; Humphreys et al. 2006; Dirksen et al. 2006; Gorbach and Portnyagin, 2011). Effect of magma mixing on volcanic glasses is expressed in shifting glass compositions to lower SiO_2 along mixing trend, as a result of direct mixing of mafic and silicic melts, or more likely along the crystallization trend due to dissolution of phenocrysts at increasing temperature. Incomplete mixing with basaltic magmas prior to eruption is also evident from a common occurrence of banded pumices and coexistence of low- and high-Si glasses in andesitic pyroclastic rocks. Effects of mixing on bulk magma composition are similar to that for glasses. Hybrid rocks have lower SiO_2 content and plot along linear mixing trends. There is also a strong effect of mixing on concentration of refractory trace elements in hybrid magmas. Gorbach and Portnyagin (2011) show that linear trends of Cr versus SiO_2 content in bulk rocks and distinctively high Cr content (>50 ppm, Ponomareva et al. 2007) in YSH tephra cannot be explained by crystallization processes but require persistent admixture of mafic Cr-rich material to Shiveluch andesites.

The processes outlined above are mainly responsible for shifting glass and/or magma compositions along (or close to) crystallization trends and unable to explain significant variability of Shiveluch glasses in K_2O content at any given SiO_2. In order to explain this variability, we propose *mixing of different geochemical type magmas*, "normal" medium-K_2O and high-K_2O, in magma-feeding system beneath Young Shiveluch. High-K_2O tephras of distinctive composition form the SHsp layer. Additional evidence for widespread involvement of high-K_2O melts comes from the presence of dacitic melt inclusions in plagioclase with up to 6.5 wt. % K_2O found in YSH rocks (Tolstykh et al. 2000). The high-K silicic melts can result from extensive crystallization of high-K basalts (SHsp tephra), crustal assimilation (Gorbach and Portnyagin 2011) or low pressure "dry" fractionation leading to stronger enrichment in K_2O compared to hydrous high pressure fractionation (e.g., Botcharnikov et al. 2008). More conclusive evidence about the origin of the K-rich component in YSH magmas can be likely obtained with the help of trace element and isotope studies.

Concurring effects of the four processes described above can readily explain the large variability of YSH glasses. These processes are rather common in the genesis of island-arc andesites (e.g., Gorbach et al. 2013 and references therein), and thus tephras of other frequently erupting andesitic volcanoes can be similarly distinguished with the help of systematic study of compositions of volcanic glass and whole rocks. Although andesitic tephra are frequently considered to be difficult for geochemical fingerprinting (Shane et al. 2005; Donoghue et al. 2007; Lowe 2011), our results provide new perspective and petrologic background for using such tephras in constraining detailed tephrostratigraphy in many volcanically active regions on continental margins.

The origin of regular temporal variations of Young Shiveluch glasses

Geochemical studies of the detailed tephra record for individual volcanoes are few (e.g., Donoghue et al. 2007; Oladottir et al. 2008; Turner et al. 2009) though they permit to study evolution of volcanoes with great details and sometimes show certain regular temporal patterns in the eruptive records (Oladottir et al. 2008). Our work at Shiveluch and Kliuchevskoi volcanoes also shows that both volcanoes exhibit wave-like changes of SiO_2 contents in glass from rapidly quenched tephras during Holocene roughly correlating in time between the volcanoes (Portnyagin et al. 2009, 2011). Both volcanoes have been erupting continuously with little (Shiveluch) or no (Kliuchevskoi) significant repose periods so their eruptions provide almost continuous temporal record of the composition of magmas (bulk rocks) and their melts (glasses) under these volcanoes.

As described in previous chapter the most profound effect on SiO_2 content in volcanic glasses have two counteracting processes, crystallization and mixing with mafic melt. Interaction between these two processes on a long time scale can provide a reasonable explanation for the wave-like pattern of SiO_2 in volcanic glass of Young Shiveluch tephra. No such clear trend is seen in the composition of bulk tephras (Fig. 11).

Low-pressure crystallization during magma transport to the surface and eruption can certainly affect the composition of volcanic glasses (e.g., Blundy et al. 2006). This process alone is, however, unlikely to result in wave-like variability of SiO_2 in Shiveluch glasses as this would imply alternating periods of more or less extensive low-pressure crystallization during the Shiveluch history without clear reason and without correlation to the magnitude of the eruptions. Alternatively, the wave-like variations can reflect the temporal evolution of melt composition in magma chamber prior to eruption and be interpreted in terms of the evolution of periodically replenished - continuously fractionated magma chamber (O'Hara 1977).

As much of the glass variations can be explained by counteracting processes of mixing and crystallization, the temporal trends from more to less silicic compositions (~11-9.9, 8.5-7.7, 5.6-4.9, 4-3 ka, and 1.5 ka-present) (Fig. 11) can be explained when mafic replenishments are frequent and/or more voluminous so that they drive melt composition in magma chamber toward more mafic one against the effect of crystallization. The opposite trend from less to more silicic compositions may imply that the effect of crystallization becomes more important and overwhelms the effect of mafic replenishments, which could be less frequent or less abundant at certain interval of time. The wave-like pattern of SiO_2 variations may thus reflect alternating periods of high and low frequency/volume of mafic magma supply to deep magma chamber beneath Shiveluch. The onsets of four of five presumed periods of high mafic magmas supply (~11-9.9, 8.5-7.7 and 4-3 ka, and 1.5 ka-present) strikingly coincide in time with known periods of enhanced volcanic activity in Kamchatka (Fig. 11) (Braitseva et al. 1995; Kozhurin et al. 2006; Pevzner et al. 2013; Ponomareva et al. 2013). This synchroneity suggests that the ascents of deeper magmas may have been caused by regional stress redistribution rather than by local processes at Shiveluch.

Implications for Shiveluch eruptive history

The activity of Shiveluch has persisted throughout the Late Glacial - Holocene times and was non-uniform in time both in terms of eruption frequency and composition of erupted products. Exclusively Baidarny-type basaltic andesite tephras were erupted between ~16 and ~12.8 ka, which represented the activity that had started in the late Pleistocene (Gorbach et al. 2013). A major divide in the Late Glacial - Holocene eruptive history was the arrival of high-Si melts at ~12.7 ka, which likely marked the onset of the YSH activity. The first small high-Si tephras might have been related to the andesitic dome- and lava-producing eruptions at the initial stages of the YSH activity (Gorbach and Portnyagin 2011; Pevzner et al. 2013). Young Shiveluch powerful explosive activity started at ~11.1 ka BP. Since then, high-Si glasses prevailed in the erupted tephras (Fig. 8).

Bulk Baidarny cinders have compositions close to Baidarny and Southern vents lavas (Fig. 7). They have significantly lower MgO, Cr and higher SiO_2, Al_2O_3, Na_2O, K_2O contents compared to the YSH unit 46 ("dark package") (Fig. 7; Online Resource 6). Glass compositions in Baidarny cinders and in the "dark package", however, are very close (Fig. 9; Online Resource 4). Melt inclusions found in minerals from Baidarny cinders and from the "dark package" have similar compositions (Pevzner et al. 2013). This implies that the "dark package" tephras are likely enriched in mafic crystals but otherwise cogenetic with Baidarny cinders and lavas. We interpret this as persisting presence (envolvement) of the Baidarny-type magmas during the YSH activity.

Conclusions

Here we present a state-of–the-art dataset of compositions and ages of Late Glacial-Holocene proximal tephras from the dominantly andesitic Shiveluch volcano (Kamchatka). The dataset is accompanied by an interactive table for comparison of unknown glasses to those from proximal tephra units (Online Resource 4). These data are used to reconstruct the eruptive history and magmatic evolution of Shiveluch during the last ~16 ka, and to assist in the identification of distal Shiveluch tephras. We explicitly envisage that our knowledge of the Shiveluch eruptive history could be updated in the future once new ^{14}C dates are added to our existing compilation and/or more tephra units are recognized and characterized geochemically.

As a result, we have obtained a nearly continuous record of glass compositions for Shiveluch tephras spanning the last ~16 ka. This record has allowed us to reveal that Young Shiveluch rhyolitic glasses exhibit wave-like variations in SiO_2 and some other elements contents through time that may reflect alternating periods of high and low frequency/volume of mafic magmas supply to deep magma chamber beneath the volcano. A wave-like pattern of SiO_2 and other elements variations through time has earlier been found for basaltic Kliuchevskoi volcano located 75 km southeast of Shiveluch (Portnyagin et al. 2009, 2011). Baidarny-type tephras were erupted mostly during the Late Glacial time (16-12.8 ka) but also persisted into the Holocene as subordinate (except for the "dark package" unit) admixture in prevailing andesitic tephras. The described compositional variability of Shiveluch glasses facilitates geochemical fingerprinting of distal Shiveluch tephras and their use as a dating tool in paleovolcanological, paleoseismological, paleoenvironmental, and archaeological studies.

At Shiveluch volcano we have encountered several well known problems related to andesitic tephra and proximal tephra sequence such as complex stratigraphy with about eighty individual pyroclastic units; similar appearance of many pumiceous tephras; high vesicularity and crystallinity of pumices and cinders; heterogeneity of glass compositions. In our case, extensive stratigraphic work (more than 200 measured sections), direct tracing of major tephra layers between the sectors, and detailed radiocarbon dating helped to compile a summary stratigraphy. A 5-µm beam size made it possible to successfully analyze even tiny glass pockets in pumices and cinders. Glass heterogeneity in some tephras, e.g., SHsp, helps to uniquely identify them.

We suggest working on proximal deposits, where available, in order to reconstruct near-continuous record of past eruptions and provide a better reference for identification and correlation of distal tephras. Dating and calibration of high resolution proximal tephrostratigraphy permit to narrow the age interval for each tephra; this refined age can be further used for more precise dating of various deposits. This research is important for the long-term forecast of eruptions and volcanic hazard assessment, and contributes to both global and regional tephra databases.

Acknowledgements. This study was supported by the Russian–German project KALMAR, funded by the German Ministry of Science and Education (BMBF), Russian Foundation for Basic Research (grant #13-05-00346) and the Otto Schmidt Laboratory for Polar and Marine Research. The large part of the samples was collected thanks to the field grant from the National Geographic Society. The authors thank Mario Thöner (GEOMAR) for the help with the microprobe analysis, and Natalia Gorbach and Sergei Khubunaya for tephra samples from AD 2001 and 2005 eruptions. Philip Kyle acknowledges support from the Division of Polar Programs, NSF (USA). Thorough reviews of two anonymous reviewers are very much appreciated.

References

Armb JT (1995) CITZAF: A package of correction programs for the quantitative electron microbeam X-ray analysis of thick polished materials, thin films, and particles. Microbeam Analysis 4:177-200

Auer S, Bindeman I, Wallace P, Ponomareva V, Portnyagin M (2009) The origin of hydrous, high-δ^{18}O voluminous volcanism: diverse oxygen isotope values and high magmatic water contents within the volcanic record of Klyuchevskoy volcano, Kamchatka, Russia. Contrib Mineral Petrol 157/2:209-230

Bazanova LI, Pevzner MM (2001) Khangar: One more active volcano in Kamchatka, Transactions (Doklady) of the Russian Academy of Sciences, Earth Sciences, 377A:307-310

Belousov A. B. (1995) The Shiveluch volcanic eruption of 12 November 1964-explosive eruption provoked by failure of the edifice. J Volcanol Geotherm Res 66:357-365

Blundy J, Cashman K (2001) Ascent-driven crystallisation of dacite magmas at Mount St Helens, 1980–1986. Contrib Mineral Petrol 140(6):631-650

Blundy J, Cashman K, Humphreys M (2006) Magma heating by decompression-driven crystallization beneath andesite volcanoes. Nature 443:76-80

Borchardt G, Aruscavage P, Millard HJ (1972) Correlation of the Bishop ash, a Pleistocene marker bed, using instrumental neutron activation analysis. J Sediment Petrol 42:301-306

Botscharnikov RE, Almeev RR, Koepcke J, Holtz F (2008) Phase relations and liquid lines of descent in hydrous ferrobasalt - Implications for the Skaergaard intrusion and Columbia River flood basalts. J Petrol 49(9):1687-1727. doi:1610.1093/petrology/egn1043

Bourgeois J, Pinegina TK, Ponomareva VV, Zaretskaia NE (2006) Holocene tsunamis in the southwestern Bering Sea, Russian Far East and their tectonic implications. The Geol Soc Amer Bull, 11 (3/4):449–463. doi: 10.1130/B25726.1

Braitseva OA, Melekestsev IV, Ponomareva VV (1983) Age divisions of the Holocene volcanic formations of the Tolbachik Valley. In: Fedotov SA (ed) The great Tolbachik fissure eruption: geological and geophysical data 1975-1976, Cambrige Earth Sci Series, pp 83-95

Braitseva OA, Florenskii IV, Ponomareva VV, Litasova SN (1989) The history of the activity of Kikhpinych volcano in the Holocene. Volcanol Seismol 7(6):845-872

Braitseva OA, Melekestsev IV, Bogoyavlenskaya GE, Maksimov AP (1991) Bezymianny volcano: eruptive history and activity dynamics. Volcanol Seismol 12(2):165-194

Braitseva OA, Sulerzhitsky LD, Litasova SN, Melekestsev IV, Ponomareva VV (1993) Radiocarbon dating and tephrochronology in Kamchatka. Radiocarbon 35:463-476

Braitseva OA, Melekestsev IV, Ponomareva VV, Sulerzhitsky LD (1995) The ages of calderas, large explosive craters and active volcanoes in the Kuril-Kamchatka region, Russia. Bull Volcanol 57(6):383-402

Braitseva OA, Ponomareva VV, Sulerzhitsky LD, Melekestsev IV, Bailey J (1997) Holocene key-marker tephra layers in Kamchatka, Russia. Quat Res 47(2):125-139

Bronk Ramsey C (2009) Bayesian analysis of radiocarbon dates. Radiocarbon 51(1):337-360

Churikova TG, Gordeichik BN, Belousov AB, Babansky AD (2010) Finding of the eruptive center for basalts at Shiveluch volcano. In: Gordeev EI (ed.) Proceedings of the All-Russia conference in honor of the 75th anniversary of the Kamchatka volcanological station. Petropavlovsk-Kamchatsky. Institute of Volcanology and Seismology FED RAS

Davaille A, Lees JM (2004) Thermal modelling of subducted plates: tear and hotspot at the Kamchatka corner. Earth Planet Sci Lett 226:293-304

Davidson J, DeSilva S (2000) Composite volcanoes. In Sigurdsson H (ed) Encyclopedia of Volcanoes: San Diego, CA, Academic Press, pp 663-682

Davies SM, Wastegård S, Rasmussen TL, Johnsen SJ, Steffensen JP, Andersen KK, Svensson A (2008) Identification of the Fugloyarbanki tephra in the NGRIP ice-core: a key tie-point for marine and ice-core sequences during the last glacial period. J Quat Sci 23:409-414

Davies SM, Abbott PM, Pearce NJG, Wastegård S, Blockley SPE (2012) Integrating the INTIMATE records using tephrochronology: rising to the challenge. Quat Sci Rev 36:11-27

Dirksen O, Humphreys MCS, Pletchov P, Melnik O, Demyanchuk Y, Sparks RSJ, Mahony S (2006) The 2001–2004 dome-forming eruption of Shiveluch volcano, Kamchatka: Observation, petrological investigation and numerical modelling. J Volcanol Geotherm Res 155:201-226

Dirksen O, van den Bogaard C, Danhara T, Diekmann B (2011) Tephrochronological investigation at Dvuh-yurtochnoe lake area, Kamchatka: Numerous landslides and lake tsunami, and their environmental impacts. Quat Int 246:298-311

Dirksen V, Dirksen O, Diekmann B (2013) Holocene vegetation dynamics in Kamchatka, Russian Far East. Rev Palaeobot Palynol 190:48–65

Donoghue SL, Vallance J, Smith IEM, Stewart RB (2007) Using geochemistry as a tool for correlating proximal andesitic tephra: case studies from Mt Rainier (USA) and Mt Ruapehu (New Zealand). J Quatern Sci 22(4):395–410

Dvigalo VN (1984) Growth of the dome in the crater of Shiveluch volcano in 1980-1981 according to photogrammetric data. Volcanol Seismol 2:104-109 (in Russian)

Eichelberger JC (1995) Silicic volcanism: Ascent of viscous magmas from crustal reservoirs. Annu. Rev. Earth Planet. Sci 23:41-63

Fedotov SA, Zharinov NA, Dvigalo VN, Seliverstov NI, Khubunaya SA (2004) The 2001-2004 eruptive cycle of Shiveluch volcano. Volcanol Seismol 6:3-14 (in Russian).

Froggatt PC (1992) Standardization of the chemical analysis of tephra deposits: report of the ICCT working group. Quat Int 13/14:93-96

Gill JB (1981) Orogenic andesites and plate tectonics. Springer-Verlag, Berlin-Heidelberg. 390 pp

Goebel T, Waters MR, Dikova M (2003) The archaeology of Ushki Lake, Kamchatka, and the Pleistocene peopling of the Americas. Science 301:501505

Gorbach NV, Portnyagin MV (2011) Geology and petrology of the lava complex of Young Shiveluch volcano (Kamchatka). Petrology 19(2):136-168

Gorbach NV, Portnyagin MV, Tembrel I (2013) Volcanic structure and composition of Old Shiveluch volcano, Kamchatka. J Volcanol Geotherm Res 263:193-208. doi: http://dx.doi.org/10.1016/j.jvolgeores.2012.12.012

Gorelchik VI, Shirokov VA, Firstov PP, Chubarova OS (1997) Shiveluch volcano: seismicity, deep structure and forecasting eruptions (Kamchatka). J Volcanol Geotherm Res 78: 21-132

Gorshkov GS, Dubik YuM (1970) Gigantic directed blast at Shiveluch volcano (Kamchatka).Bull Volcanol 34:261-288

Hulse EL, Keeler DM, Zubrow EBW, Korosec GJ, Ponkratova IY, Curtis C (2011) A preliminary report on archaeological fieldwork in the Kamchatka Region of Russia. Sibirica 1:48-74

Humphreys MCS, Blundy JD, Sparks RSJ (2006) Magma evolution and open-system processes at Shiveluch Volcano: Insights from phenocryst zoning. J Petrol 47 (12):2303-2334. doi: 10.1093/petrology/egl045

Humphreys MCS, Blundy JD, Sparks RSJ (2008) Shallow-level decompression crystallisation and deep magma supply at Shiveluch Volcano. Contrib Mineral Petrol 155(1):45-61

Jarosewich EJ, Nelen JA, Norberg JA (1980) Reference samples for electron microprobe analysis. Geostandards Newsletter, 4:43-47

Khubunaya SA, Zharinov NA, Muravyev YaD, Ivanov VV, Boloyavlenskaya GE, Novgorodtseva TYu, Demyanchuk YuV, Budnikov VA, Fazlullin S. M. (1995) 1993 eruption of Shiveluch volcano. Volcanol Seismol 17:1-20

Kirianov VYu, Egorova IA, Litasova SN (1990) Volcanic ash on Bering Island (Commander Islands) and Kamchatkan Holocene eruptions. Volcanol Seismol 8:850-868

Kozhurin A, Acocella V, Kyle PR, Lagmay FM, Melekestsev IV, Ponomareva VV, Rust D, Tibaldi A, Tunesi A, Corazzato C, Rovida A, Sakharov A, Tengonciang A, Uy H (2006) Trenching active faults in Kamchatka, Russia: paleoseismological and tectonic implications. Tectonophysics 417:285-304

Kozhurin AI, Pinegina TK, Ponomareva VV, Zelenin EA, Mikhailyukova PG (2014) Rate of collisional deformation in Kamchatsky Peninsula, Kamchatka Geotectonics 48(2):122-138

Kuehn SC, Froese DG, Shane PAR (2011) The INTAV intercomparison of electron-beam microanalysis of glass by tephrochronology laboratories: Results and recommendations. Quat Int, 246:19-47. doi:10.1016/j.quaint.2011.08.022

Kyle PhR, Ponomareva VV, Rourke Schluep R (2011) Geochemical characterization of marker tephra layers from major Holocene eruptions in Kamchatka, Russia. Int Geol Rev 53(9):1059–1097

Le Bas MJ, Le Maitre r W, Streckeisen A, Zanettin B (1986) A chemical classification of volcanic rocks based on the total alkali-silica diagram. J Petrol 27:745–750

Lowe DJ (2011) Tephrochronology and its application: A review. Quat Geochronol 6:107-153

Melekestsev IV, Volynets ON, Ermakov VA, Kirsanova TP, Masurenkov YuP (1991) Shiveluch volcano. In: Fedotov SA, Masurenkov YuP (eds) Active volcanoes of Kamchatka, vol 1. Nauka Press, Moscow, pp 84-103

Melekestsev IV, Kurbatov AV (1998) Frequency of large paleoearthquakes at the northwestern coast of the Bering Sea and in the Kamchatka basin during late Pleistocene/Holocene time. Volcanol Seismol 19:257-267

Mosbah M, Metrich N, Massiot P (1991) PIGME fluorine determination using a nuclear microprobe with application to glass inclusions. Nucl Instrum Methods B58:227-231

O'Hara MJ (1977) Geochemical evolution during fractional crystallization of a periodically refilled magma chamber. Nature 266:503-507

Oladottir B, Sigmarsson O, Larsen G, Thordarson T (2008) Katla volcano, Iceland: magma composition, dynamics and eruption frequency as recorded by Holocene tephra layers. Bull Volcanol 70 (4):475-493

Pendea IF, Ponomareva V, Bourgeois J, Korosec G, LaSelle S-P, Ponkratova I, Ferguson C, Fraser R, Keeler D, Zubrow E (2012) Late Glacial to Holocene Environmental History of eastern Kamchatka Peninsula, North Pacific. Abstracts of the Geological Association of Canada Conference, May 2012, St John's, NL.

Peacock MA (1931) Classification of igneous rocks. J Geol 39:54-67

Pevzner MM (2003) Tephrostratigraphic reference layers in the Holocene soil sections of the southern part of the Sredinny Range and some peculiarities in ^{14}C dating of the peats. Volcanol Seismol 4:1-15

Pevzner MM (2010) The northern boundary of volcanic activity of Kamchatka in Holocene. Bulletin of Kamchatka Regional Association "Educational-scientific Center". Earth Sciences. 1/15:231-258 [In Russian] http://www.kscnet.ru/kraesc/2010/2010_15/2010_15_eng.html

Pevzner MM, Ponomareva VV, Melekestsev IV (1998) Chernyi Yar - reference section of the Holocene ash markers at the northeastern coast of Kamchatka. Volcanol Seismol 19(4):389-406

Pevzner MM, Babansky AD (2011) Basaltic activity episode at 4600-3100 ^{14}C years BP (3370-1400 cal BC) at andesitic Shiveluch volcano, Kamchatka. Abstracts of the International Biennial Workshop on Subduction Processes emphasizing the Japan-Kurile-Kamchatka-Aleutian Arcs (JKASP). Petropavlovsk-Kamchatsky, Russia, August 25-30. P. 262-263

Pevzner MM, Tolstykh ML, Babansky AD, Kononkova NN (2013) Reconstruction of the magmatic system in the Shiveluch volcanic massif as a result of large-scale collapses of its edifice in the late Pleistocene-early Holocene. Doklady Earth Sciences 448 (1):35-37

Pevzner MM, Tolstykh ML, Babansky AD, Layer P., Volynets A.O. (2014) First data on the isotope age and composition of the parental melts of the initial stage of the Shiveluch volcanic massif. Volcanism and associated processes. Materials of the annual conference celebrating the Volcanologist Day. Petropavlovsk-Kamchatsky, Institute of Volcanology and Seismology, pp 104-107 http://www.kscnet.ru/ivs/publication/volc_day/2014/art16.pdf [In Russian]

Pinegina TK, Kozhurin AI, Ponomareva VV (2012) Seismic and tsunami hazard for Ust'-Kamchatsk village, Kamchatka, based on paleoseismological data. Bulletin of Kamchatka Regional Association "Educational-scientific Center". Earth Sciences. 1/19:138-159 [In Russian] http://www.kscnet.ru/kraesc/2012/2012_19/2012_19_eng.html

Ponomareva VV (1990) The history of Krasheninnikov volcano and the dynamics of its activity. Volcanol Seismol 9:714-741

Ponomareva VV, Pevzner MM, Melekestsev IV (1998) Large debris avalanches and associated eruptions in the Holocene eruptive history of Shiveluch Volcano, Kamchatka, Russia. Bull Volcanol 59:490-505

Ponomareva VV, Kyle PR, Pevzner MM, Sulerzhitsky LD, Hartman M (2007) Holocene eruptive history of Shiveluch volcano. Kamchatka Peninsula. In: Eichelberger J, Gordeev E, Kasahara M, Izbekov P, Lees J (eds) Volcanism and Subduction: The Kamchatka Region, American Geophysical Union Geophysical Monograph Series, American Geophysical Union, Washington DC, vol 172, pp 263-282

Ponomareva VV, Portnyagin MV, Melnikov DV (2012) Composition of tephra from modern (2009-2011) eruptions of the Kamchatka and Kuril Islands volcanoes. Bulletin of Kamchatka Regional Association "Educational-scientific Center". Earth Sciences. 2/20:7-21 [In Russian] http://www.kscnet.ru/kraesc/2012/2012_20/2012_20_eng.html

Ponomareva V, Portnyagin M, Derkachev A, Pendea IF, Bourgeois J, Reimer PJ, Garbe-Schönberg D, Krasheninnikov S, Nürnberg D (2013) Early Holocene M~6 explosive eruption from Plosky volcanic massif (Kamchatka) and its tephra as a link between terrestrial and marine paleoenvironmental records. J Int Earth Sci 102(6):1673-1699. doi: 10.1007/s00531-013-0898-0

Portnyagin M, Bindeman I, Hoernle K, Hauff F (2007) Geochemistry of primitive lavas of the Central Kamchatka Depression: Magma Generation at the Edge of the Pacific Plate. In: Eichelberger J, Gordeev E, Kasahara M, Izbekov P, Lees J (eds) Volcanism and Subduction: The Kamchatka Region, American Geophysical Union Geophysical Monograph Series, American Geophysical Union, Washington DC, vol 172, pp 199-239

Portnyagin M, Ponomareva V, Bindeman I, Hauff F, Krasheninnikov S, Kuvikas O, Mironov N, Pletchova A, van den Bogaard C, Hoernle K (2009) Millennial variations of major and trace element and isotope compositions of Klyuchevskoy magmas, Kamchatka. Terra Nostra 1:64-65

Portnyagin M, Mironov N, Ponomareva V, Bindeman I, Hauff F, Sobolev A, Kayzar T, Garbe-Schönberg D, Hoernle K (2011) Arc magmas from slab to eruption: the case of Kliuchevskoy volcano. Mineralogical Magazine. Abstracts of the 2011 Goldcshmidt Conference, Prague, p 1661; http://www.minersoc.org

Portnyagin M, Hoernle K, Mironov NL (2012) Contrasting compositional trends of rocks and olivine-hosted melt inclusions from Cerro Negro volcano (Central America): implications for decompression-driven fractionation of hydrous magmas. Int J Earth Sci. doi: 10.1007/s00531-012-0810-3

Reimer PJ, Bard E, Bayliss A, Beck JW, Blackwell PG, Bronk Ramsey C, Buck CE, Cheng H, Edwards RL, Friedrich M, Grootes PM, Guilderson TP, Haflidason H, Hajdas I, Hatté1 C, Heaton TJ, Hoffmann DL, Hogg AG, Hughen KA, Kaiser KF, Kromer B, Manning SW, Niu M, Reimer RW, Richards DA, Scott EM, Southon JR, Staff RA, Turney CSM, van der Plicht J (2013) IntCal13 and Marine13 Radiocarbon Age Calibration Curves 0-50,000 Years cal BP. Radiocarbon 55(4):1869-1887

Shane P, Nairn IA, Smith VC (2005) Magma mingling in the ~50 ka Rotoiti eruption from Okataina Volcanic Centre: implications for geochemical diversity and chronology of large volume rhyolites. J Volcanol Geotherm Res 139:295-313

Tolstykh ML, Naumov VB, Babanskii AD et al. (2000) Chemical composition, trace elements, and volatile components of melt inclusions in minerals from andesites of the Shiveluch Volcano, Kamchatka. Geochem Int 38 (Suppl 1):S123-S132

Turner M, Bebbington M, Cronin S, Stewart R (2009) Merging eruption datasets: building an integrated Holocene eruptive record for Mt Taranaki, New Zealand. Bull Volcanol 71(8):903-918

Volynets ON (1979) Heterotaxitic lavas and pumices and the problem of magma mixing. In: Sobolev VS (Ed.) Problems of Deep Magmatism, pp 181–197, Nauka Press, Moscow (in Russian)

Volynets ON, Ponomareva VV, Babansky AD (1997) Magnesian basalts of Shiveluch andesite volcano, Kamchatka. Petrology 5(2):183-196

Zharinov NA, Bogoyavlenskaya GE, Khubunaya SA, Demyanchuk YuV (1995) A new eruption cycle of Shiveluch volcano, 1980-1993. Volcanol Seismol 17:21-30

Zharinov NA, Demyanchuk YuV (2013) Large explosive eruptions of Shiveluch volcano, Kamchatka resulting in partial destruction of the extrusive dome (February 28, 2005 and October 27, 2010). J Volcanol Seismol 7(2):131-144

Table 1 Comparison of glass compositions from major Kamchatka tephras to Shiveluch proximal data

Figure captions

Fig. 1 Shiveluch volcanic massif seen from southwest. Inset shows the location of Shiveluch volcano (yellow star) in relation to major tectonic features: Aleutian arc to the east and Kuril-Kamchatka arc to the south

Fig. 2 Satellite image of Shiveluch volcanic massif consisting of the late Pleistocene Old Shiveluch (Old SH) volcano, destroyed by a collapse crater, and the currently active Young Shiveluch (YSH) eruptive center nested in the latter. Southwestern part of Old Shiveluch (Baidarny Spur) is formed by lava flows from Baidarny and Southern vents marked with blue diamonds. Red diamonds show positions of the Holocene Shiveluch vents. A tuff ring at the southwestern slope of Baidarny Spur produced a large tephra (the "dark package", see text for discussion). Yellow circles show positions of tephra sections with analyzed tephra samples. Small black circles show all measured sections in the area. River valleys mentioned in the text are labeled in white. Numbers around the frame show north-based directions from the Young Shiveluch crater used for determining the tephra fall axes (Online Resource 4)

Fig. 3 Typical outcrops of the Holocene tephra sequence on the Shiveluch slopes. **a** - tephra sequence overlying pyroclastic density current deposits in Mutny Creek valley, northwestern slope of the Shiveluch edifice, 13.5 km from the modern dome; **b** - major pumice fall layers in Dry Ilchinets valley, southeastern sector of Shiveluch slope, 12 km from the modern dome. Labels of major tephra units as in Fig. 5, Online Resources 1-4. SHsp and SHdv are important YSH marker tephras discussed in the text. Marker tephra layers from other volcanoes: KHG (~7.85 ka) – Khangar; KZ (~8.1 ka; highlighted with a yellow line) - Kizimen; PL2 (~10.2 ka) and PL1 (~11 ka) – Plosky volcanic massif

Fig. 4 Outcrops of Late Glacial – Holocene deposits in Dry Ilchinets valley (southeastern sector of Shiveluch slope, 11 km from the modern dome). **a-b** - Holocene tephra sequence overlying two debris avalanche deposits (DAD), and Late Glacial sequence sandwiched between them; **c** - Late Glacial tephra sequence between the two DADs. The lower part of the sequence contains only gray or oxidized Baidarny cinders (coarse and fine sands, and rare lapilli). The upper part (transition package labeled TP, see text for discussion) is dominated by 0.5-3 cm thick layers of white very fine silicic ash related to the onset of the Young Shiveluch active period (~12.7 ka BP) but also contains a few thin layers of Baidarny cinders. Numbers of the analyzed samples from this outcrop are shown left and right of the photo; black and yellow labels show samples taken in 1996 and 2011, respectively. Radiocarbon dates (Pevzner et al. 2013) are shown in red. Dates within each box have been obtained on different fractions of the same sample

Fig. 5 Simplified summary stratigraphy of the Late Glacial-Holocene pyroclastic sequence on the Shiveluch slopes. Deposits from individual YSH eruptions (in this paper referred to as units) are shown with boxes and labeled left of those. Large tephras (bulk volumes ca. >0.5 km^3) are highlighted in yellow. Small tephras forming the "transition package" are shown with green dotted lines and labeled T1-T5 (from top to bottom). Late Glacial Baidarny tephras are combined into four packages (B1-B4) highlighted in blue. In some cases (units 23 - 27b and the bottom of the YSH sequence) we were not able to correlate deposits from different slopes of the volcano, therefore we show the stratigraphies from each slope separately. Pyroclastic material analyzed in this paper is indicated inside each box: f - tephra fall deposits, i - ignimbrite. Units 17, 26, 31, and 38 marked "n/a" have not been analyzed because the samples were not available. In units 7 and 9 marked "n/d" no fresh glass has been detected. Codes for marker tephra layers from Shiveluch used in previous research are the same as in Ponomareva et al. (2007) and are labeled in magenta left and right of the boxes. "Lower yellow" is one of the marker tephra layers from Shiveluch identified in this paper. Regional marker tephra layers are shown with thick magenta lines and labeled in magenta, from top to bottom: BZ1956 – Bezymianny volcano AD 1956 tephra; KS_1 and KS_2 – Ksudach volcano tephra (Braitseva et al. 1995, 1997); KL – Kliuchevskoi (Braitseva et al. 1995); KHG – Khangar (Bazanova and Pevzner 2001); KZ – Kizimen (Braitseva et al. 1997); PL1 and PL2 - Plosky volcanic massif (Ponomareva et al. 2013). Calibrated ages of the Shiveluch pyroclastic units and regional marker tephra layers (weighted mean of all age estimates for each layer) are given right of the boxes or magenta lines. Direction of dispersal for large tephras is provided right of the ages. The lower age boundary for the Late Glacial part of the Shiveluch tephra sequence (15.8-16 ka) is based on calculations of soil accumulation rate (Pevzner et al. 2013). For complete summary stratigraphy and analyzed samples IDs see Online Resource 1

Fig. 6 Backscattered electron images of selected Shiveluch tephra. **a-c -** Young Shiveluch pumiceous tephra: **a** - SH_1 (unit 4, sample 757-1), **b** - SH2800 (unit b, sample 775-8), **c** – early Holocene high-K pumice (sample 775-25); **d-f** – cinders: **d** – SHsp (unit 28, sample 757-20); **e** - "dark package" (unit 46, sample K01-17); **f -** Baidarny cinder (sample 97057-3). For stratigraphic position of the samples see Online Resource 1

Fig. 7 Compositions of Shiveluch lava and proximal lapilli tephra. In TAS plot fields shown according to Le Bas et al (1986): B – basalt, BA – basaltic andesite, A – andesite, D – dacite, BTA – basaltic trachyandesite, TA - trachyandesite, TD – trachydacite. In K_2O - SiO_2 plot low-, medium-, and high-K fields are shown after Gill (1981). Data on tephra are from Ponomareva et al. (2007) and this study, and data on lava compositions are from Gorbach and Portnyagin (2011) and Gorbach et al. (2013). The labels on the diagrams indicate two basalt - basaltic andesite tephras (SHsp and "dark package") discussed in the text

Fig. 8 Histograms of SiO_2 contents in glasses from tephra erupted at different stages of Late Glacial-Holocene Shiveluch activity show that glass compositions fall into two major groups: glasses from Baidarny and YSH cinders have ~58-71.5 wt. % SiO_2 (low-Si glasses), and glasses from YSH pumices are mostly rhyolitic with SiO_2=71.5-80 wt. % (high-Si glasses). Dotted gray line shows the boundary between the two groups

Fig. 9 Compostions of Shiveluch glasses plotted versus SiO_2 content. Small gray dots in background illustrate a compositional range of glasses from Holocene Kamchatka tephras (Kyle et al. 2011; Ponomareva et al. 2012, 2013; V. Ponomareva and M. Portnyagin, unpublished). Fields of different rock types in TAS (see Fig. 7 for abbreviations) and K_2O vs. SiO_2 plots are shown after Le Bas et al. (1986) and Gill (1981), respectively. Error bars (2sigma) characterize 95% uncertainty of individual data points as calculated from multiple standard measurements by propagating the errors to the average composition of Shiveluch glass. The labels on the diagrams indicate two basalt - basaltic andesite tephras (SHsp and "dark package") discussed in the text

Fig. 10 Examples of homogeneous (**a**) and heterogeneous (**b**) glass compositions found in different YSH pumice units (color circles). Labels of the units have same colors as the symbols for corresponding glass compositions, and are the same as in Fig. 5 and Online Resources). For the units used as markers in previous research (e.g., Braitseva et al. 1997;

Pevzner et al. 1998; Kyle et al. 2011) their codes are provided in brackets. Gray circles show glass compositions in all the YSH tephra

Fig. 11 Temporal variations in SiO_2 and K_2O contents in Shiveluch glasses and bulk lapilli during Late Glacial – Holocene times. Dotted gray line at 71.5% SiO_2 shows the boundary between low-Si and hi-Si glasses. Gray shaded bars show the periods of enhanced volcanic activity in Kamchatka (Braitseva et al. 1995; Kozhurin et al. 2006; Pevzner et al. 2013; Ponomareva et al. 2013)

Fig. 12 Comparison of Shiveluch glass compositions to those from other large Holocene Kamchatka tephras (see discussion in the text). Fields and averages for glass compositions from different tephras from Kyle et al. (2011) and Ponomareva et al. (2013). A map (**d**) shows sources of the largest Holocene Kamchatka tephras. Tephra codes: AV_1, IAV2 - Avachinsky volcano; IL - Iliinsky volcano; KHD - Khodutkinsky crater; KHG -Khangar volcano; KO - Kurile Lake caldera; KRM - Karymsky caldera; KS_1, KS_2, KS_3, $KSht_3$ - Ksudach eruptive center; KZ - Kizimen volcano; OP - Barany Amphitheater crater at Opala volcano; OPtr - Chasha crater; PL - Plosky eruptive center

Fig. 13 Minimum dispersal of selected YSH tephras based on new correlations with distal sites. Color circles show locations of the analyzed distal tephra samples. Ovals of matching colors show minimum dispersal areas for tephra units 56, 59, and 58 ("Lower yellow"). Findings of YSH tephras in the marine cores SO201-2-81 and SO201-2-77 are the first ever findings of Shiveluch tephra in the marine sediments, which allow us to estimate the minimum dispersal of Holocene Shiveluch tephra at 560-580 km. Inset shows the location of Attu Island, where tephra samples attributed by Kyle et al. (2011) to Shiveluch likely come from another source (see text for discussion)

Fig. 14 Results of comparison of glass compositions in distal tephras with the proximal YSH high-Si glasses. **a** - "Lower yellow" (LY) tephra was used as a marker in the Eastern Kamchatka but its source was not known because its composition did not match then known YSH ones (Kyle et al. 2011). Comparison of LY glass to our proximal data shows that it matches early Holocene YSH tephras. **b** - SH_5 tephra is one of the markers from YSH dispersed to the south of the volcano earlier dated at ~2550 ^{14}C yrs based on erroneous correlation to unit 24 (Ponomareva et al. 2007). Comparison of the glass data for distal and proximal tephras have allowed us to correlate the distal tephra to YSH unit 21 dated at ~1850 cal BP. **c** - glass compositions of tephras found in the Bering Sea cores SO201-2-77KL and -81KL in association with the PL2 marker tephra (~10.2 ka; Plosky eruptive center) suggest their correlation to proximal early Holocene YSH units 56 and 59. **d -** glasses from the three tephras found on Attu Island and attributed to Shiveluch (Kyle et al. 2011) form a single group and have lower K_2O contents than the majority of the YSH glasses

Online Resource 1 Schematic summary section through Late Glacial - Holocene Shiveluch pyroclastic sequence

Online Resource 2 OxCal code used for calibrating the sequence of radiocarbon dates obtained for the Shiveluch pyroclastic deposits

Online Resource 3 Calibrated ages of the Shiveluch tephra units and marker tephra layers from other volcanoes

Online Resource 4 Compilation of data on Shiveluch glass compositions and statistical tools for their comparison

Online Resource 5 Electron microprobe analyses of glass from distal Shiveluch tephras mentioned in the paper

Online Resource 6 Chemical analyses of bulk tephra used in this paper

Table 1. Comparison of glass compositions from major Kamchatka tephras to Shiveluch proximal data

Tephra ID	Source volcano	Glass compositions compared to those from Shiveluch	Additional characteristics different from the Shiveluch ones
AV_1, IAV2	Avachinsky	Very different: lower K_2O and Na_2O; higher CaO and Ca/Na_2O+K_2O	
IL	Iliinsky	Very different: lower K_2O, Na_2O and TiO_2; higher CaO, FeO, MgO and Ca/Na_2O+K_2O	
KHD	Khodutkinsky Crater	Different: lower K_2O	
KHG	Khangar	Different: lower Na_2O and lower Cl	Presence of mica
KO	Kurile Lake caldera	Very different: lower K_2O; higher CaO, FeO and Ca/Na_2O+K_2O	
KRM	Karymsky caldera	Different: lower Na_2O and Al_2O_3; higher FeO and Cl	Absence of hornblende
$KSht_3$, KS_1, KS_2, KS_3	Ksudach	Very different: low K_2O; higher CaO and Ca/Na_2O+K_2O	Absence of hornblende
KZ	Kizimen	Different: lower Na_2O and higher CaO	
OP	Barany Amphitheater Crater, Opala volcano	Different: higher K_2O; lower FeO, MgO and TiO_2	Presence of mica
OPtr	Chasha Crater	Different: higher K_2O; lower Na_2O, FeO, MgO, TiO_2 and Cl	Presence of mica
PL1,PL2, PL3	Plosky volcanic massif	Very different: higher K_2O and P_2O_5; lower Na_2O and Cl	

The table includes major Holocene Kamchatka tephras studied for glass compositions by Kyle et al. (2011) and Ponomareva et al. (2013). Source volcanoes are listed from north to south. “Very different” implies that the contents of the listed oxides do not overlap with those from Shiveluch. “Different” means that the contents of the listed oxides are close to Shiveluch compositions but still differ from the majority of those. Glass compositions from listed tephras are shown on the diagrams (Fig. 12).

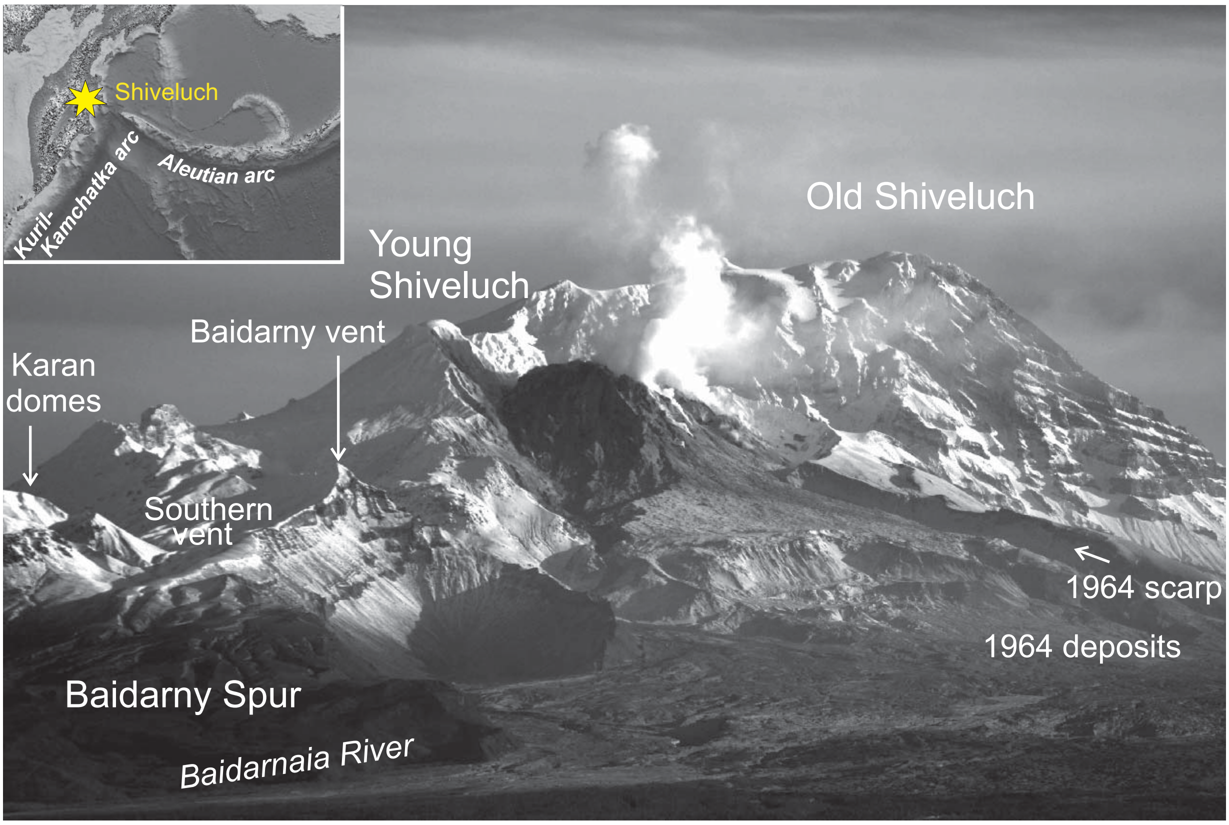
Shiveluch
Kuril-
Kamchatka arc
Aleutian arc
Old Shiveluch
Young
Shiveluch
Baidarny vent
Karan
domes
Southern
vent
1964 scarp
1964 deposits
Baidarny Spur
Baidarnaia River

Fig. 1

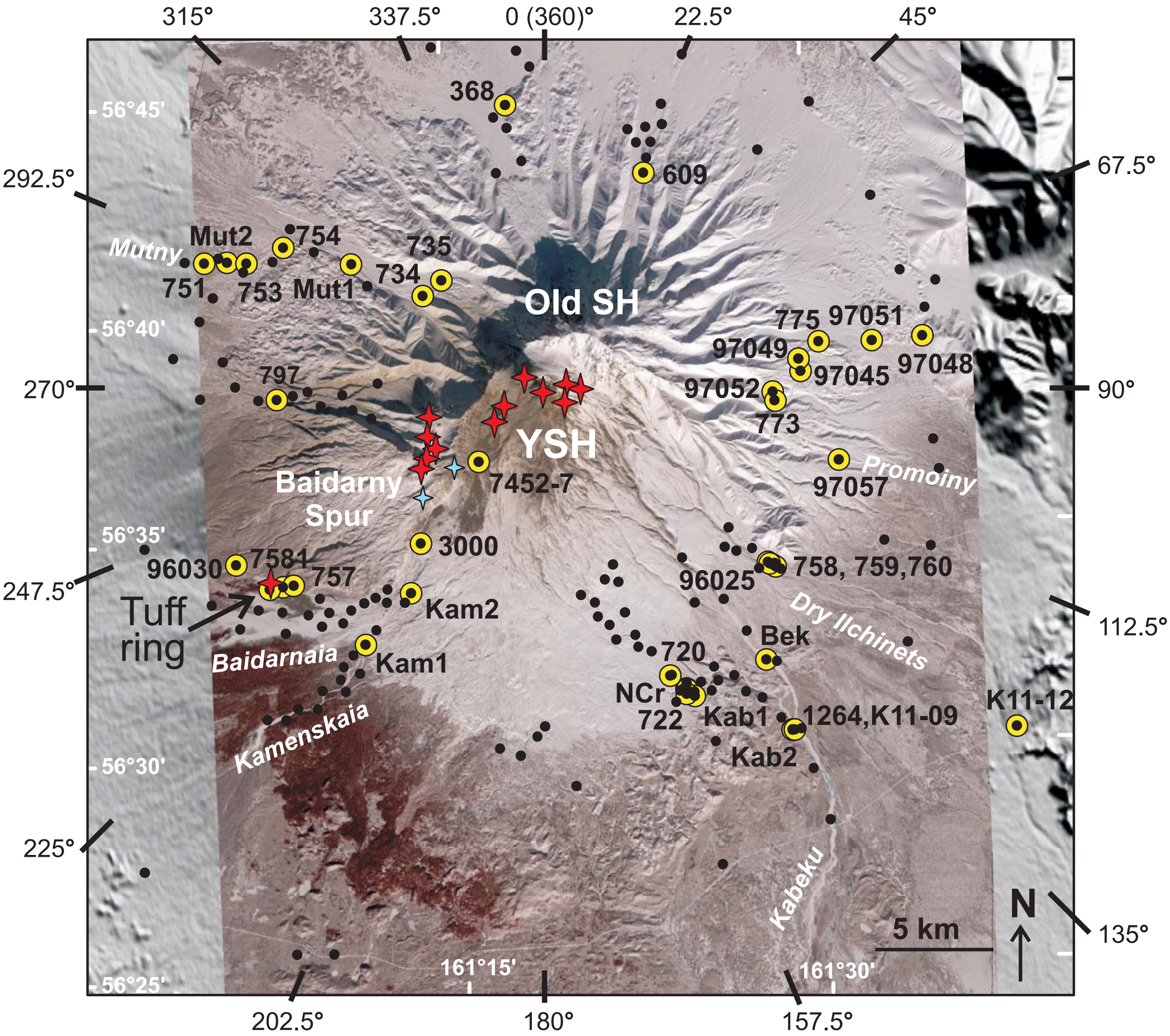

315°
337.5°
0 (360)°
22.5°
45°
67.5°
292.5°
270°
90°
247.5°
112.5°
225°
135°
202.5°
180°
157.5°
56°45'
56°40'
56°35'
56°30'
56°25'
161°15'
161°30'
368
609
Mut2
754
735
Mutny
751
753
Mut1
734
Old SH
775
97051
97049
97048
97045
97052
773
797
YSH
7452-7
97057
Promoiny
Baidarny Spur
3000
96030
7581
757
96025
758, 759,760
Tuff ring
Kam2
Dry Ilchinets
Baidarnaia
Kam1
720
Bek
NCr
722
Kab1
1264,K11-09
K11-12
Kamenskaia
Kab2
Kabeku
5 km
N

Fig. 2


a
25
SHsp 28
31?
SHdv 34
35
b
36
37
42
KHG
KZ
46
47
48
51
52
55
56
PL2
PL1
61

Fig. 3

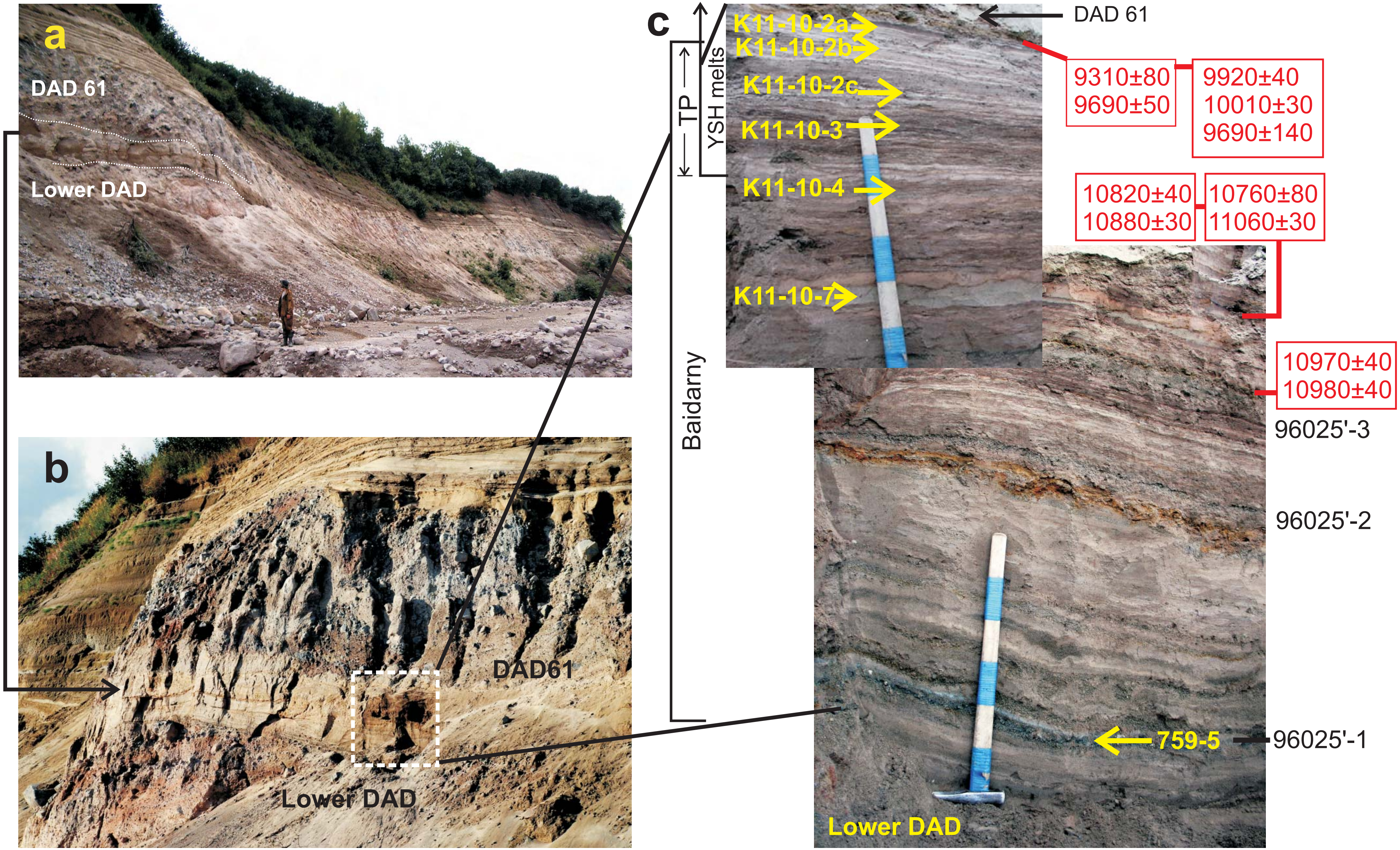
a
DAD 61
Lower DAD
b
DAD61
Lower DAD
c
TP
YSH melts
Baidarny
K11-10-2a
K11-10-2b
K11-10-2c
K11-10-3
K11-10-4
K11-10-7
DAD 61
9310±80
9690±50
9920±40
10010±30
9690±140
10820±40
10880±30
10760±80
11060±30
10970±40
10980±40
96025'-3
96025'-2
96025'-1
759-5
Lower DAD

Fig. 4

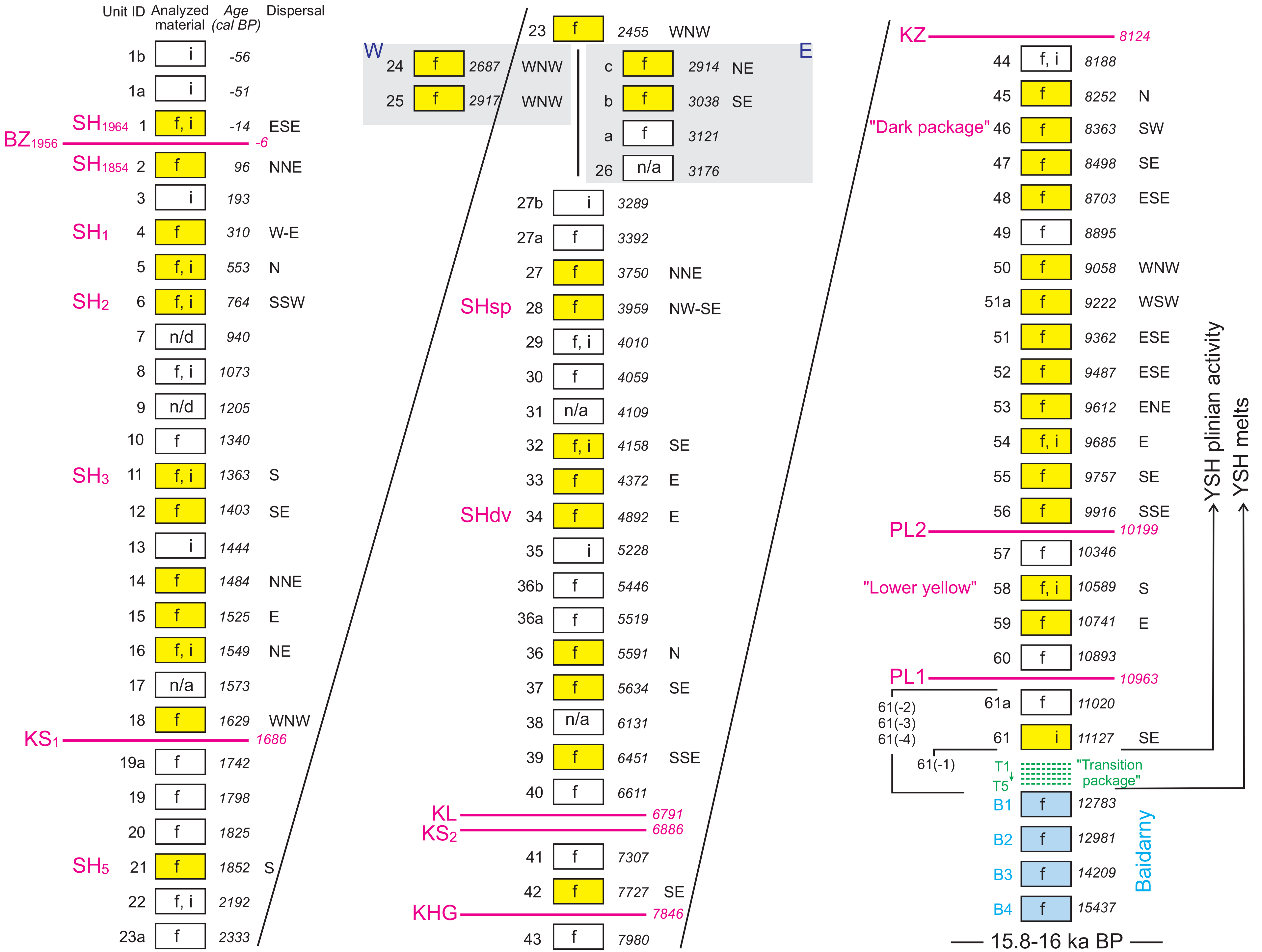

Unit ID Analyzed material Age (cal BP) Dispersal
1b i -56
1a i -51
SH1964 1 f, i -14 ESE
BZ1956 -6
SH1854 2 f 96 NNE
3 i 193
SH1 4 f 310 W-E
5 f, i 553 N
SH2 6 f, i 764 SSW
7 n/d 940
8 f, i 1073
9 n/d 1205
10 f 1340
SH3 11 f, i 1363 S
12 f 1403 SE
13 i 1444
14 f 1484 NNE
15 f 1525 E
16 f, i 1549 NE
17 n/a 1573
18 f 1629 WNW
KS1 1686
19a f 1742
19 f 1798
20 f 1825
SH5 21 f 1852 S
22 f, i 2192
23a f 2333
23 f 2455 WNW
W
24 f 2687 WNW
25 f 2917 WNW
E
c f 2914 NE
b f 3038 SE
a f 3121
26 n/a 3176
27b i 3289
27a f 3392
27 f 3750 NNE
SHsp 28 f 3959 NW-SE
29 f, i 4010
30 f 4059
31 n/a 4109
32 f, i 4158 SE
33 f 4372 E
SHdv 34 f 4892 E
35 i 5228
36b f 5446
36a f 5519
36 f 5591 N
37 f 5634 SE
38 n/a 6131
39 f 6451 SSE
40 f 6611
KL 6791
KS2 6886
41 f 7307
42 f 7727 SE
KHG 7846
43 f 7980
KZ 8124
44 f, i 8188
45 f 8252 N
"Dark package" 46 f 8363 SW
47 f 8498 SE
48 f 8703 ESE
49 f 8895
50 f 9058 WNW
51a f 9222 WSW
51 f 9362 ESE
52 f 9487 ESE
53 f 9612 ENE
54 f, i 9685 E
55 f 9757 SE
56 f 9916 SSE
PL2 10199
57 f 10346
"Lower yellow" 58 f, i 10589 S
59 f 10741 E
60 f 10893
PL1 10963
61a f 11020
61(-2)
61(-3)
61(-4)
61 i 11127 SE
61(-1)
T1
T5
"Transition package"
B1 f 12783
B2 f 12981
B3 f 14209
B4 f 15437
Baidarny
YSH plinian activity
YSH melts
15.8-16 ka BP

Fig. 5

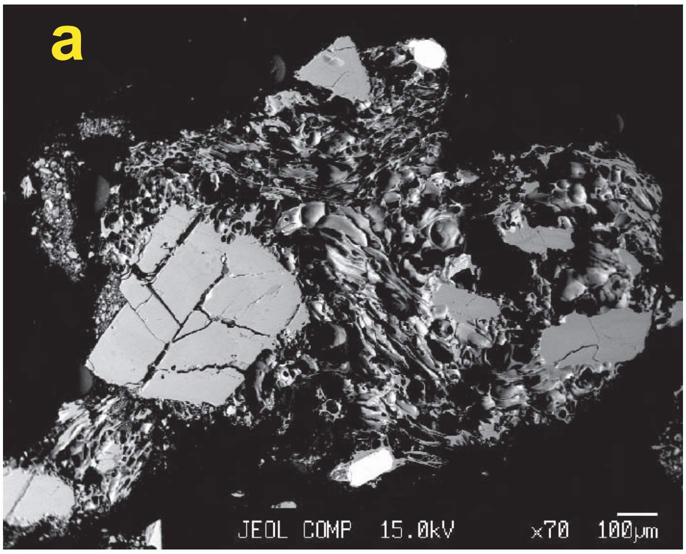

YSH unit 4, SH_1, 757-1

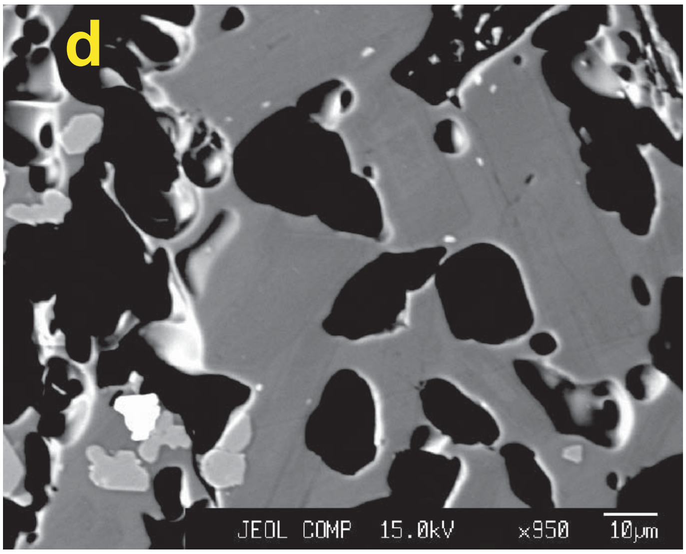

YSH unit 28, SHsp, 757-20

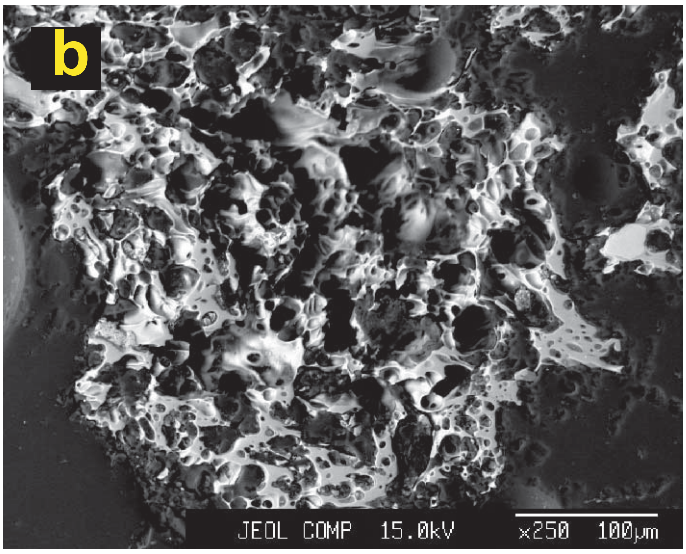

YSH unit b, SH2800, 775-8

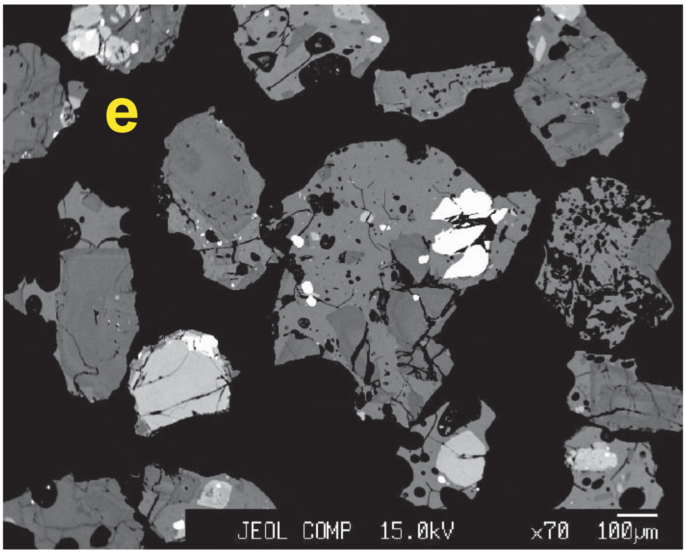

YSH unit 46, Dark package, K01-17

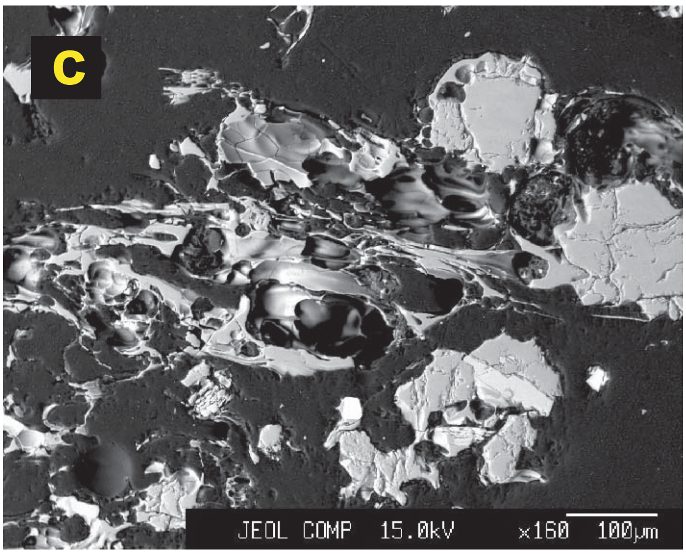

YSH, 775-25

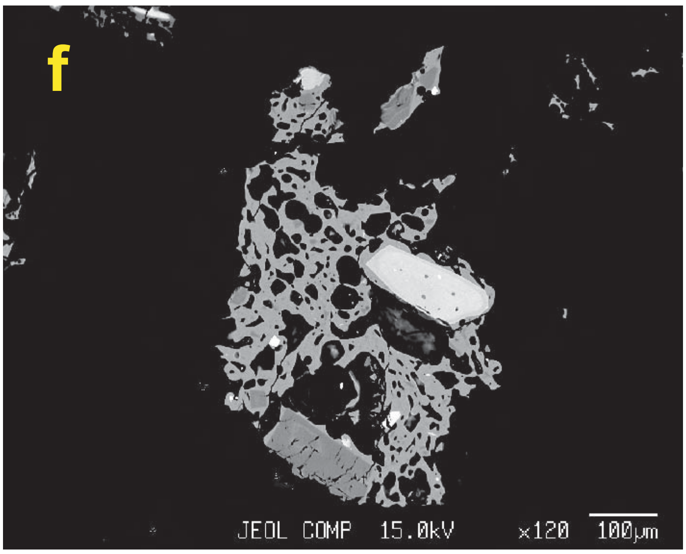

Baidarny, 97057-3

Fig. 6

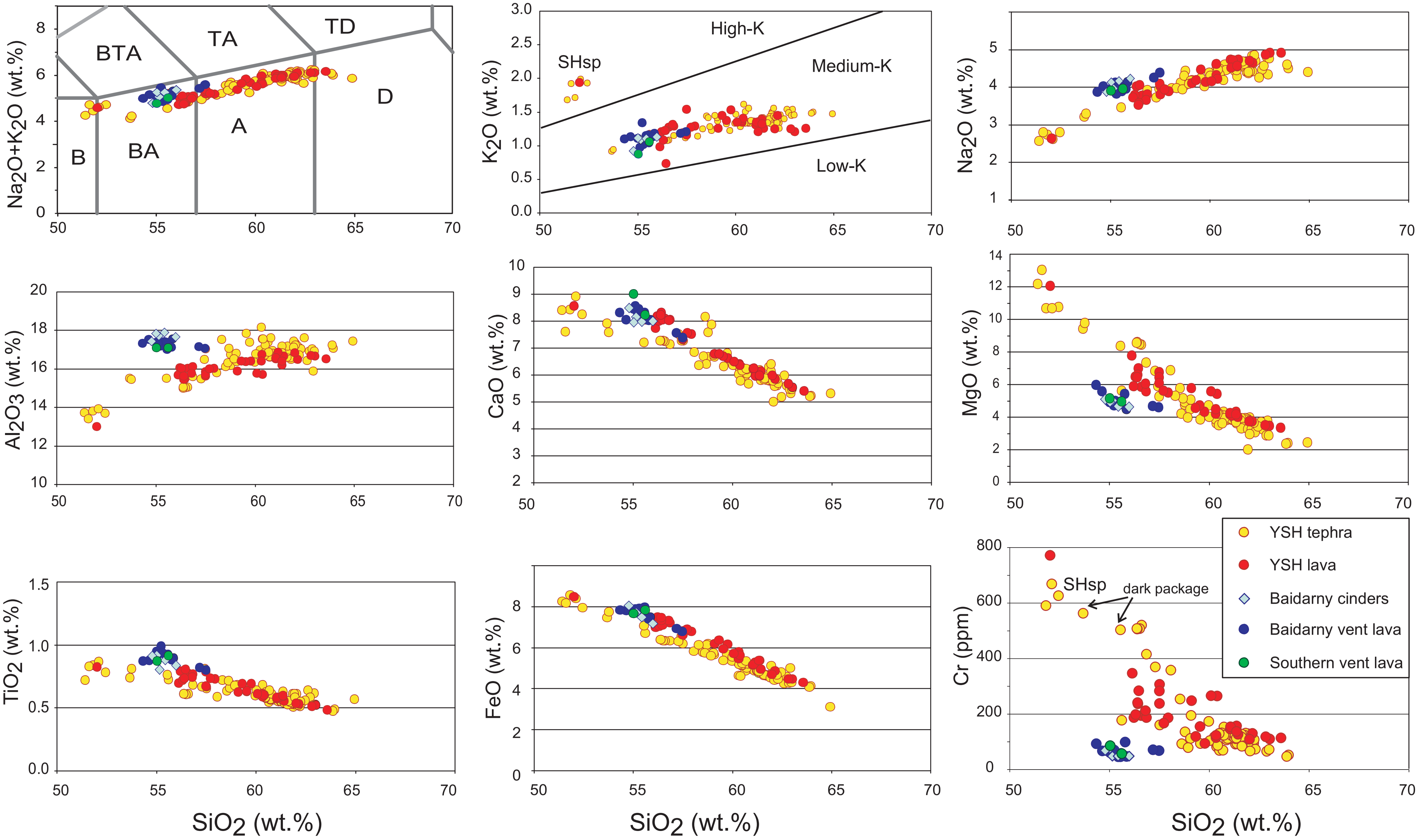

Na2O+K2O (wt.%)
B
BA
BTA
TA
A
TD
D
K2O (wt.%)
SHsp
High-K
Medium-K
Low-K
Na2O (wt.%)
Al2O3 (wt.%)
CaO (wt.%)
MgO (wt.%)
TiO2 (wt.%)
FeO (wt.%)
Cr (ppm)
SHsp
dark package
YSH tephra
YSH lava
Baidarny cinders
Baidarny vent lava
Southern vent lava
SiO2 (wt.%)
SiO2 (wt.%)
SiO2 (wt.%)

Fig. 7

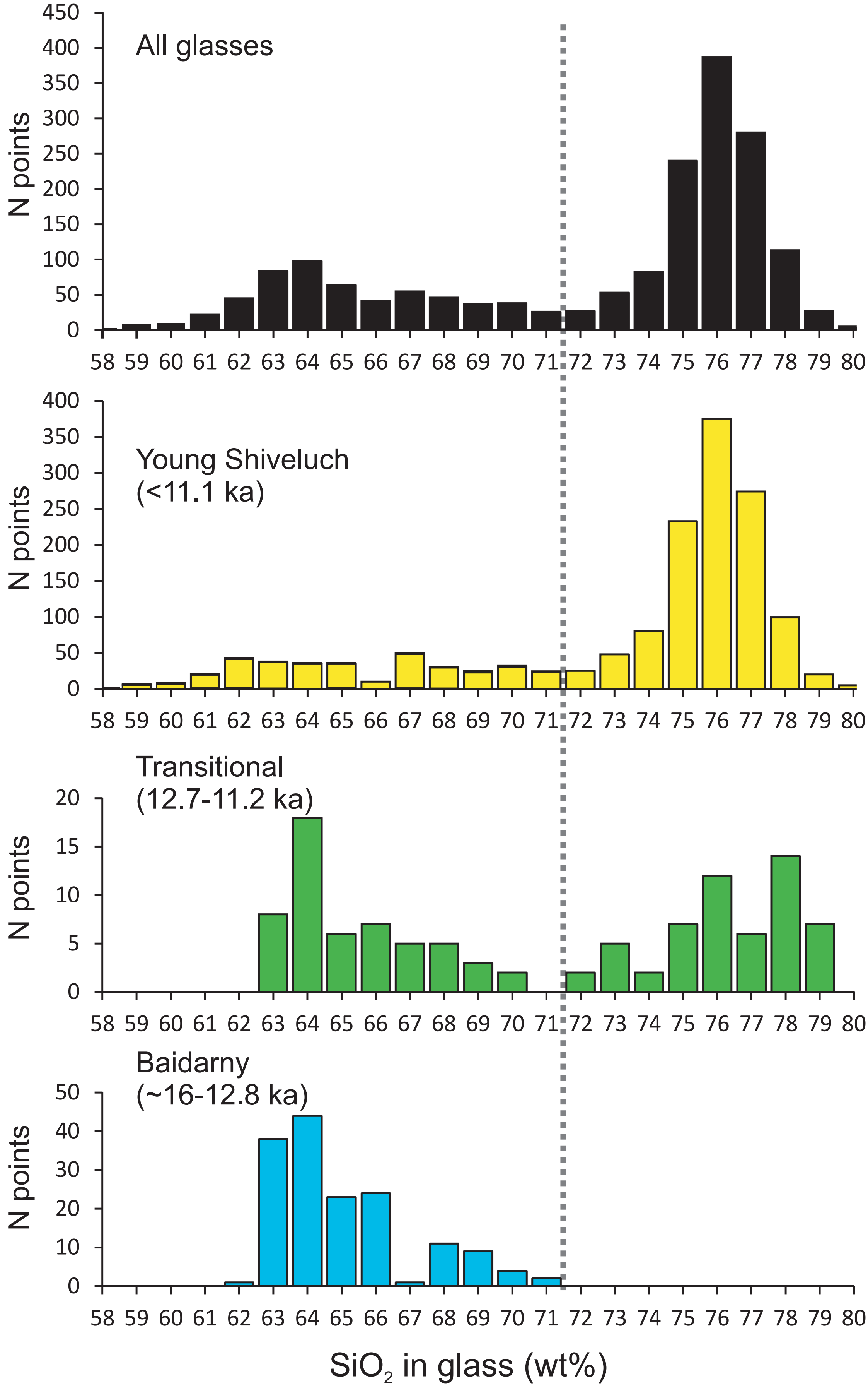
All glasses
Young Shiveluch
(<11.1 ka)
Transitional
(12.7-11.2 ka)
Baidarny
(~16-12.8 ka)
N points
SiO2 in glass (wt%)
58 59 60 61 62 63 64 65 66 67 68 69 70 71 72 73 74 75 76 77 78 79 80
0 50 100 150 200 250 300 350 400 450
0 5 10 15 20
0 10 20 30 40 50

Fig. 8

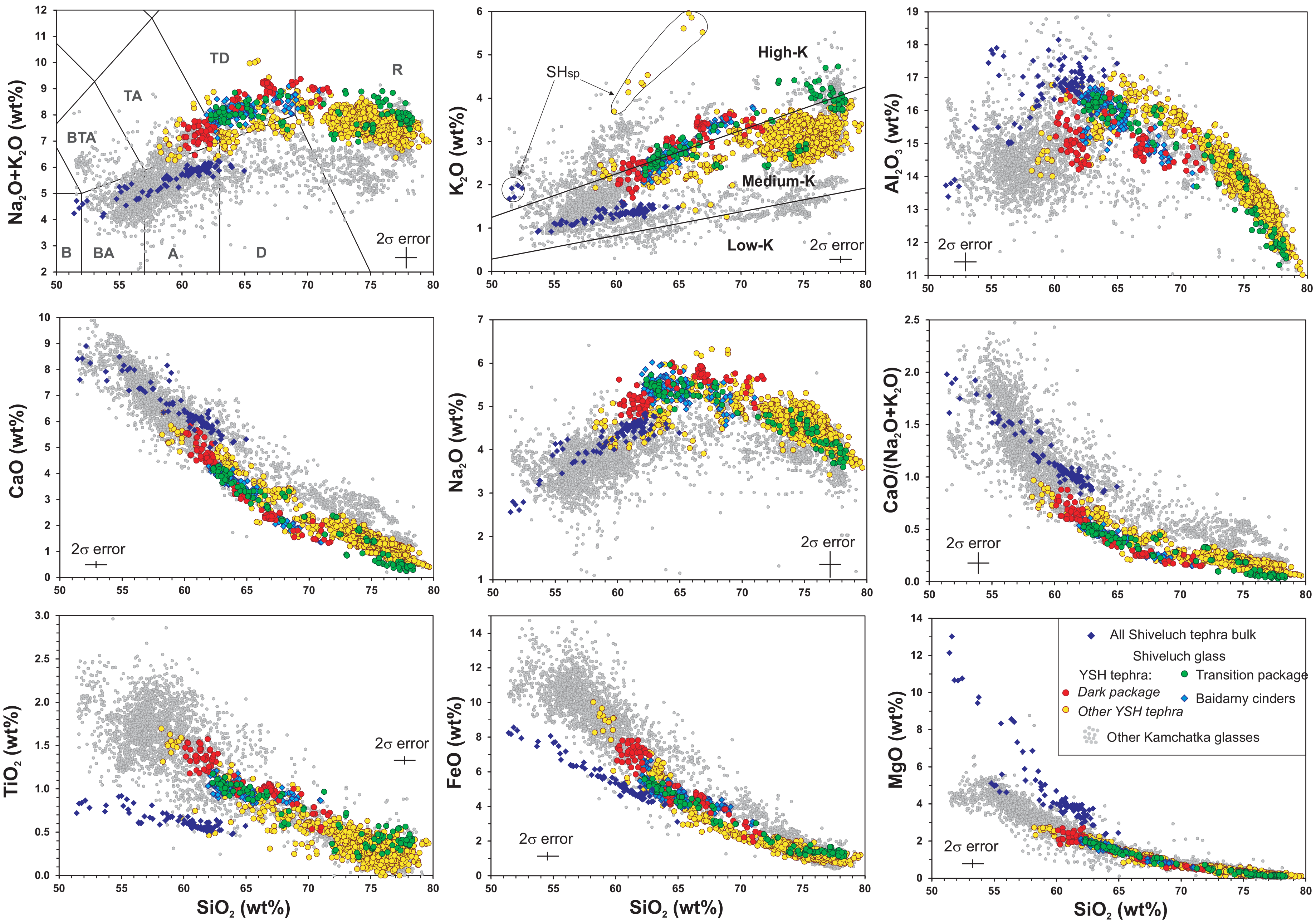
Na2O+K2O (wt%)
TD
R
TA
BTA
B
BA
A
D
2σ error
K2O (wt%)
SHsp
High-K
Medium-K
Low-K
Al2O3 (wt%)
CaO (wt%)
Na2O (wt%)
CaO/(Na2O+K2O)
TiO2 (wt%)
FeO (wt%)
MgO (wt%)
SiO2 (wt%)
All Shiveluch tephra bulk
Shiveluch glass
YSH tephra:
Dark package
Other YSH tephra
Transition package
Baidarny cinders
Other Kamchatka glasses

Fig. 9

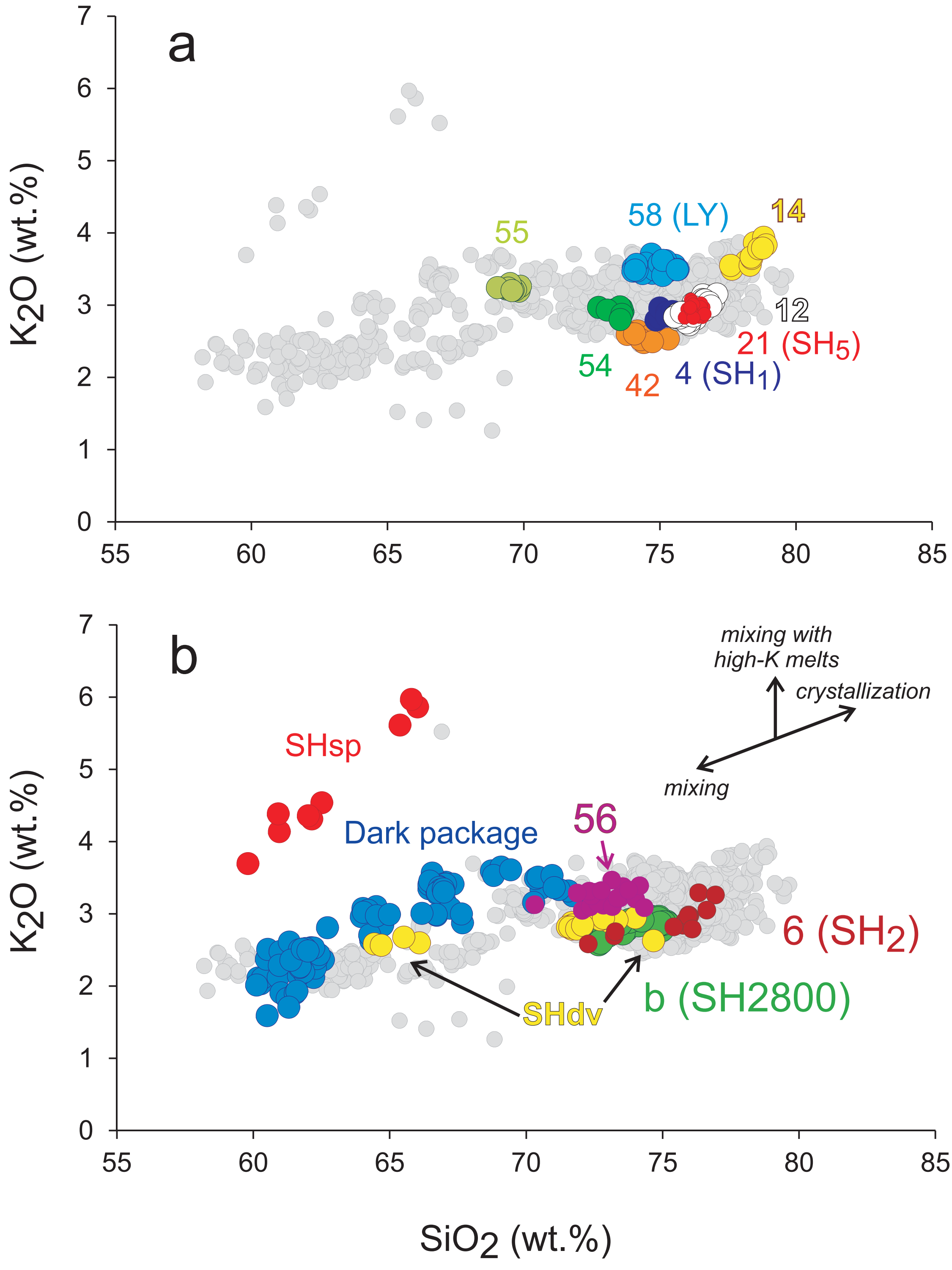

a
K2O (wt.%)
55
58 (LY)
14
12
21 (SH5)
54
42
4 (SH1)
b
mixing with
high-K melts
crystallization
mixing
SHsp
Dark package
56
6 (SH2)
SHdv
b (SH2800)
SiO2 (wt.%)

Fig.10

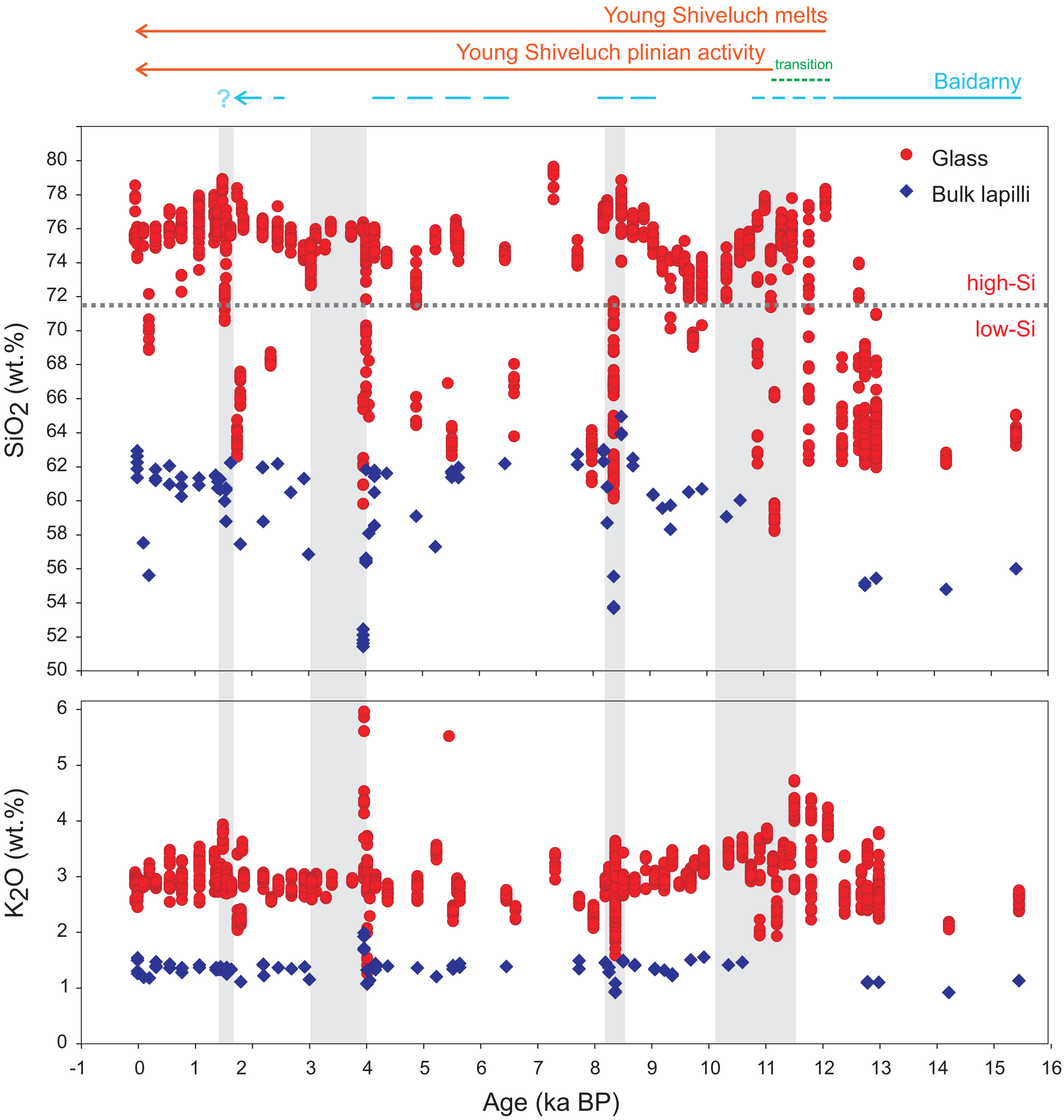

Young Shiveluch melts
Young Shiveluch plinian activity
transition
Baidarny
?
Glass
Bulk lapilli
high-Si
low-Si
SiO2 (wt.%)
80
78
76
74
72
70
68
66
64
62
60
58
56
54
52
50
K2O (wt.%)
6
5
4
3
2
1
0
-1
0
1
2
3
4
5
6
7
8
9
10
11
12
13
14
15
16
Age (ka BP)

Fig. 11

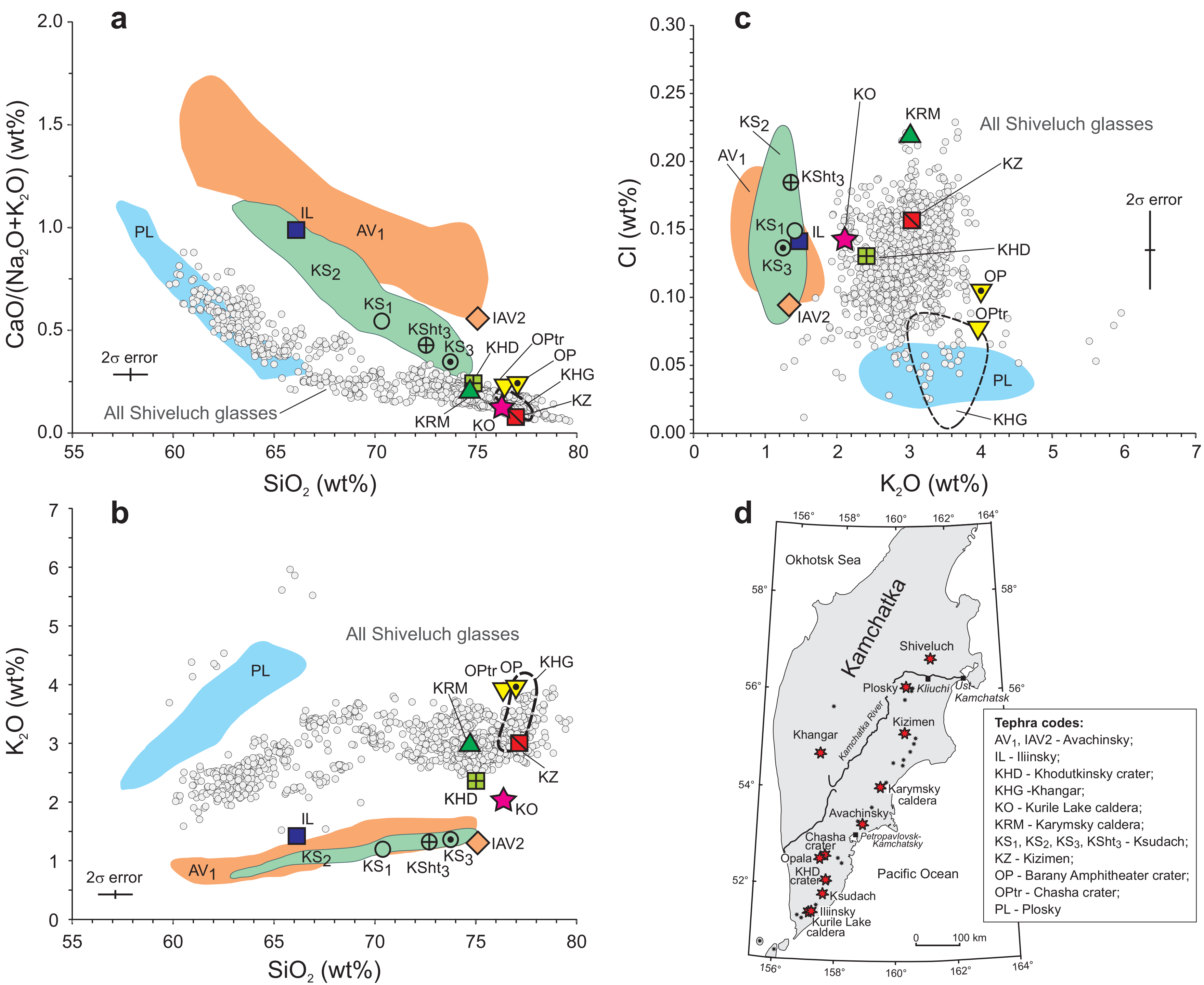
a
CaO/(Na2O+K2O) (wt%)
SiO2 (wt%)
All Shiveluch glasses
2σ error
PL
IL
AV1
KS2
KS1
KSht3
KS3
KHD
OPtr
OP
KHG
KZ
KO
KRM
IAV2
b
K2O (wt%)
SiO2 (wt%)
All Shiveluch glasses
2σ error
c
Cl (wt%)
K2O (wt%)
All Shiveluch glasses
2σ error
d
Okhotsk Sea
Kamchatka
Shiveluch
Plosky
Kliuchi
Ust-Kamchatsk
Kizimen
Khangar
Kamchatka River
Karymsky caldera
Avachinsky
Petropavlovsk-Kamchatsky
Chasha crater
Opala
KHD crater
Ksudach
Iliinsky
Kurile Lake caldera
Pacific Ocean
100 km
Tephra codes:
AV1, IAV2 - Avachinsky;
IL - Iliinsky;
KHD - Khodutkinsky crater;
KHG -Khangar;
KO - Kurile Lake caldera;
KRM - Karymsky caldera;
KS1, KS2, KS3, KSht3 - Ksudach;
KZ - Kizimen;
OP - Barany Amphitheater crater;
OPtr - Chasha crater;
PL - Plosky

Fig. 12

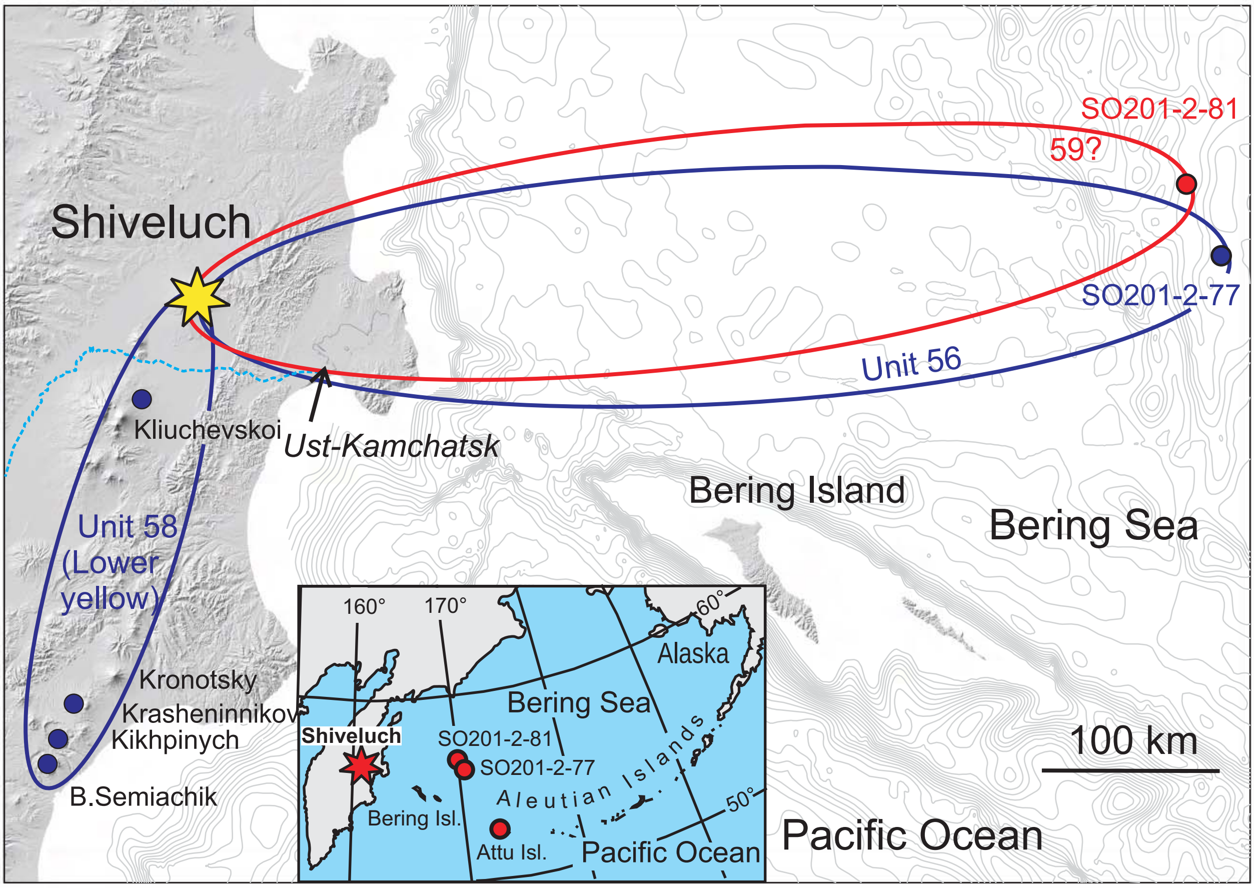

Shiveluch
SO201-2-81
59?
SO201-2-77
Unit 56
Kliuchevskoi
Ust-Kamchatsk
Bering Island
Bering Sea
Unit 58
(Lower
yellow)
Kronotsky
Krasheninnikov
Kikhpinych
B.Semiachik
160°
170°
60°
Alaska
Bering Sea
Shiveluch
SO201-2-81
SO201-2-77
Aleutian Islands
Bering Isl.
50°
Attu Isl.
Pacific Ocean
100 km
Pacific Ocean

Fig. 13

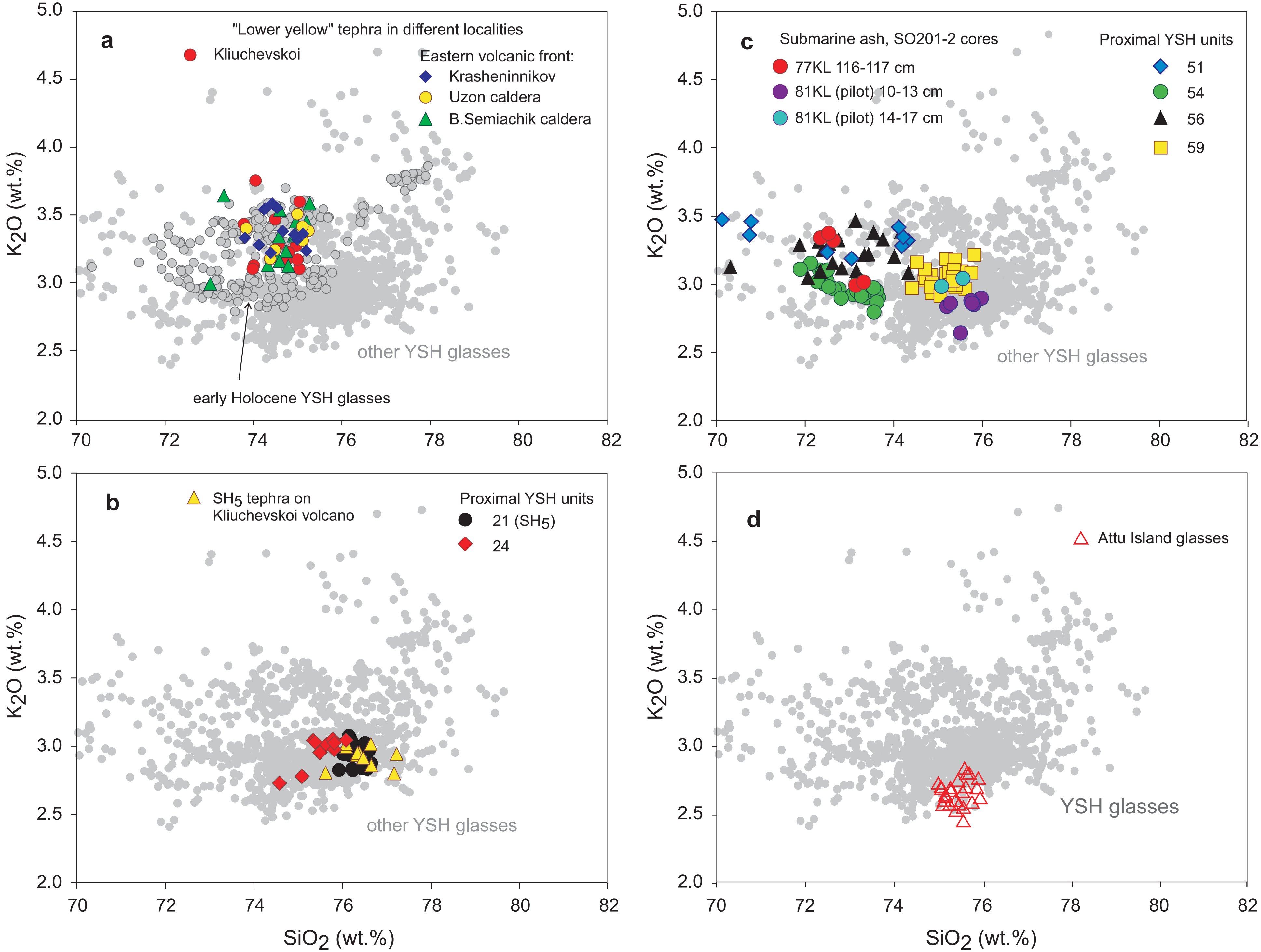

a
"Lower yellow" tephra in different localities
Kliuchevskoi
Eastern volcanic front:
Krasheninnikov
Uzon caldera
B.Semiachik caldera
early Holocene YSH glasses
other YSH glasses
b
SH5 tephra on
Kliuchevskoi volcano
Proximal YSH units
21 (SH5)
24
other YSH glasses
c
Submarine ash, SO201-2 cores
77KL 116-117 cm
81KL (pilot) 10-13 cm
81KL (pilot) 14-17 cm
Proximal YSH units
51
54
56
59
other YSH glasses
d
Attu Island glasses
YSH glasses
K2O (wt.%)
SiO2 (wt.%)

Fig. 14